

LOCKING-FREE HYBRID HIGH-ORDER METHOD FOR LINEAR ELASTICITY

CARSTEN CARSTENSEN AND NGOC TIEN TRAN

ABSTRACT. The hybrid-high order (HHO) scheme has many successful applications including linear elasticity as the first step towards computational solid mechanics. The striking advantage is the simplicity among other higher-order nonconforming schemes and its geometric flexibility as a polytopal method on the expanse of a parameter-free refined stabilization. This paper utilizes just one reconstruction operator for the linear Green strain and therefore does not rely on a split in deviatoric and spherical behaviour as in the classical HHO discretization. The a priori error analysis provides quasi-best approximation with λ -independent equivalence constants. The reliable and (up to data oscillations) efficient a posteriori error estimates are stabilization-free and λ -robust. The error analysis is carried out on simplicial meshes to allow conforming piecewise polynomials finite elements in the kernel of the stabilization terms. Numerical benchmarks provide empirical evidence for optimal convergence rates of the a posteriori error estimator in some associated adaptive mesh-refining algorithm also in the incompressible limit, where this paper provides corresponding assertions for the Stokes problem.

1. INTRODUCTION

1.1. Motivation. The first HHO elasticity model has been analyzed in [23] with emphasis on general meshes and two different recovery operators for the linear Green strain and for the divergence of the displacements. The a priori error analysis therein provides λ -robust convergence rates relative to the possibly restricted elliptic regularity on polygons with general boundary conditions of changing type. The first paper on the HHO in nonlinear elasticity [8] suggests an HHO method with one recovery operator for the linear Green strain tensor. Optimal convergence rates in [23, 26] under unrealistic regularity assumptions on the exact solutions are *not* visible for quasi-uniform triangulations in typical benchmark problems of computational mechanics.

The analysis of this paper departs from λ -robust quasi-best approximation results for the L^2 stress error [16, 14, 33] in discrete problems with a smoother [40, 41, 29, 15] or without (and then up to data oscillations for L^2 source terms). A first benefit is the validity of the error estimates under minimal regularity assumptions. A second benefit arises in the efficiency of the stabilization – a stepping stone towards stabilization-free a posteriori error control [4] that is of interest in the convergence analysis of adaptive mesh-refining algorithms [43]. A duality argument and [20] lead to L^2 estimates for the displacement beyond typical model problems on convex domains with pure Dirichlet boundary conditions [11, 28]. While HHO methods

Date: 13th December 2024.

2010 Mathematics Subject Classification. 65N12, 65N30, 65Y20.

Key words and phrases. linear elasticity, hybrid high-order, error estimates, a priori, a posteriori.

The authors thank Lukas Gehring (Universität Jena) for his valuable comments that lead to the completion of the proof of Lemma 3.6.

The second author received funding from the European Union’s Horizon 2020 research and innovation programme (project RandomMultiScales, grant agreement No. 865751).

can be defined on polytopal meshes, the error analysis of this paper exploits the orthogonality of the stress error with conforming test functions. Therefore, it is restricted to regular triangulations into simplices. Other contributions [5, 36] on stabilized schemes allow polygonal meshes in the derivation of a posteriori error estimators but avoid a λ -robustness analysis.

1.2. Mathematical model. Let $\Omega \subset \mathbb{R}^n$ with $n = 2, 3$ be a bounded polyhedral Lipschitz domain in two or three space dimensions with boundary $\partial\Omega$ that is split into a closed Dirichlet part $\Gamma_D \subset \partial\Omega$ of positive surface measure and a remaining Neumann part $\Gamma_N := \partial\Omega \setminus \Gamma_D$. Given $f \in L^2(\Omega)^n$ and $g \in L^2(\Gamma_N)^n$, the model problem in linear elasticity of this paper seeks the solution $u \in H^1(\Omega)^n$ to

$$(1.1) \quad -\operatorname{div} \sigma = f \text{ in } \Omega, \quad \sigma := \mathbb{C}\varepsilon(u), \quad u = 0 \text{ on } \Gamma_D, \quad \sigma\nu = g \text{ on } \Gamma_N.$$

The linearized Green strain $\varepsilon(v) := \operatorname{sym}(Dv)$ is the symmetric part of the gradient Dv and the isotropic elasticity tensor \mathbb{C} acts as $\mathbb{C}\tau := 2\mu\tau + \lambda\operatorname{tr}(\tau)\mathbf{I}_{n \times n}$ for any $\tau \in L^2(\Omega)^{n \times n}$ with the Lamé parameters $\lambda \geq 0$ and $\mu > 0$. We assume that, for $|\Gamma_N| > 0$, the parameters λ, μ are piecewise constant such that μ is bounded away from zero $0 < \mu_0 \leq \mu \leq \mu_1$ by positive numbers $\mu_0 \leq \mu_1$ and, for $|\Gamma_N| = 0$, λ and μ are positive constants. The weak formulation seeks the solution $u \in V := \{v \in H^1(\Omega)^n : v = 0 \text{ on } \Gamma_D\}$ to

$$(1.2) \quad \int_{\Omega} \mathbb{C}\varepsilon(u) : \varepsilon(v) \, dx = \int_{\Omega} f \cdot v \, dx + \int_{\Gamma_N} g \cdot v \, ds \quad \text{for all } v \in V.$$

1.3. Main results. The HHO methodology [24, 23, 26] allows for a reconstruction operator $\mathcal{G} : V_h \rightarrow P_k(\mathcal{T})^{n \times n}$ of the gradient from a discrete ansatz space V_h of V onto the space $P_k(\mathcal{T})^{n \times n}$ of matrix-valued piecewise polynomials of degree at most k . The approximation $\mathbb{C}\varepsilon_h$ of $\mathbb{C}\varepsilon$ with $\varepsilon_h := \operatorname{sym} \mathcal{G}$ does not rely on a split in deviatoric and spherical behavior as in [23]. This was proposed in [8] and the HHO method therein seeks the solution $u_h \in V_h$ to

$$a_h(u_h, v_h) = F_h(v_h) \quad \text{for any } v_h \in V_h$$

with a scalar product a_h in V_h and bounded linear functional F_h . The reconstruction operator ε_h leads to a straight-forward definition of the discrete stress $\sigma_h := \mathbb{C}\varepsilon_h u_h$ with the L^2 orthogonality $\sigma - \sigma_h \perp \varepsilon(P_{k+1}(\mathcal{T})^n \cap V)$. The latter allows for the application of the tr-div-dev lemma in the error analysis for λ -robust estimates. We establish, up to data oscillations, the quasi-best approximation

$$(1.3) \quad \begin{aligned} & (\mu_0/\mu_1)^{1/2} \|\sigma - \sigma_h\| + \mu_0^{1/2} \|\mathbf{I}u - u_h\|_{a_h} + \mu_0^{1/2} |u_h|_s \\ & \leq C_{\text{qb}} (\|(1 - \Pi_{\mathcal{T}}^k)\sigma\| + \operatorname{osc}(f, \mathcal{T}) + \operatorname{osc}(g, \mathcal{F}_N)) \end{aligned}$$

under a mild assumption on the geometry, where $\mathbf{I} : V \rightarrow V_h$ is the canonical interpolation in the HHO methodology, $\|\bullet\|_{a_h}$ is the norm induced by a_h , $|\bullet|_s$ is the seminorm induced by the stabilization, and $\Pi_{\mathcal{T}}^k$ is the L^2 projection onto piecewise polynomials. Notice that (1.3) holds under minimal regularity assumption on u , while [23, 26] requires at least piecewise H^s regularity of the stress σ for some $s > 1/2$, which is not available for boundary conditions of changing type on a straight line. The proof of (1.3) utilizes the arguments of [29, 4] but additionally requires a quasi-best approximation result for the stabilization in the spirit of [21]. Duality techniques allow for L^2 error estimates with additional convergence rates depending on the elliptic regularity on polyhedral domains. If $f \in H^{-1}(\Omega)^n$ and $g \in \tilde{H}^{-1/2}(\Gamma_N)^n$ are nonsmooth, a modified HHO solver with a smoother [40, 41, 29, 15] is proposed with an oscillation-free version of (1.3).

The a posteriori error analysis combines the techniques from the residual and equilibrium error estimation of [4]. We establish

$$(1.4) \quad C_{\text{rel}}^{-1}(\mu_0/\mu_1)\|\sigma - \sigma_h\| \leq \eta \leq C_{\text{eff}}(\mu_1/\mu_0)(\|\sigma - \sigma_h\| + \text{osc}(f, \mathcal{T}) + \text{osc}(g, \mathcal{F}_N)).$$

with the error estimator

$$(1.5) \quad \eta^2 := \|h_{\mathcal{T}}(f + \text{div}_{\text{pw}}\sigma_h)\|^2 + \min_{v \in V} \|\mu(\varepsilon(v) - \varepsilon_h u_h)\|^2 + \sum_{F \in \mathcal{F}(\Omega)} h_F \|[\sigma_h]_{F\nu_F}\|_{L^2(F)}^2 + \sum_{F \in \mathcal{F}_N} h_F \|g - \sigma_h \nu_F\|_{L^2(F)}^2.$$

All the constants C_{qb} , C_{rel} , C_{eff} , and those throughout this paper (unless explicitly stated otherwise) do not depend on λ , μ , and the mesh size. In the computations, we chose $v = \mathcal{A}u_h$ in (1.5) with the nodal average $\mathcal{A}u_h$ of the potential reconstruction $\mathcal{R}u_h$ of u_h . This choice is efficient as a non-trivial generalization to [4] for the Poisson model problem.

1.4. Outline. The remaining parts of this paper are organized as follows. Section 2 introduces the discrete problem with the aforementioned reconstruction operators and stabilization. Quasi-best approximation and L^2 error estimates follow in Section 3. Section 4 derives reliable and efficient a posteriori error estimates. Computational benchmarks in Section 5 provide numerical evidence for λ -robustness.

1.5. General notation. Standard notation for Sobolev and Lebesgue spaces applies throughout this paper. In particular, $(\bullet, \bullet)_{L^2(\Omega)}$ denotes the L^2 scalar product and induces the norm $\|\bullet\| := \|\bullet\|_{L^2(\Omega)}$ in $L^2(\Omega)$ and any product $L^2(\Omega)^n$ or $L^2(\Omega)^{n \times n}$ thereof. The norm $\|\bullet\|_{-1}$ in the dual space $H^{-1}(\Omega)$ of $H_0^1(\Omega)$ reads

$$(1.6) \quad \|F\|_{-1} := \sup_{v \in H_0^1(\Omega) \setminus \{0\}} F(v) / \|\nabla v\|.$$

For any $\Phi, \Psi \in L^2(\Omega)^{n \times n}$ and $s \in \mathbb{R}$, abbreviate $(\Phi, \Psi)_{\mathbb{C}^s} := (\mathbb{C}^s \Phi, \Psi)_{L^2(\Omega)}$ and $\|\Psi\|_{\mathbb{C}^s}^2 := (\Psi, \Psi)_{\mathbb{C}^s}$. The symmetric and asymmetric part of the gradient Dv of some function v are denoted by $\varepsilon(v) := \text{sym}(Dv)$ and $D_{\text{ss}}v := \text{asym}(Dv)$ with the formula $\text{sym}(M) := (M + M^t)/2$ and $\text{asym}(M) := (M - M^t)/2$ for any $M \in \mathbb{R}^{n \times n}$. For Sobolev functions $v \in H^1(\Omega)^n$, the Korn inequality

$$(1.7) \quad \|v\|_{H^1(\Omega)} \leq C_K \|\varepsilon(v)\|$$

holds subject to different constraints to fix the rigid body motions. For $v \in V$, (1.7) is referred as the first Korn inequality with a constant C_K that exclusively depends on Ω and Γ_D . The second Korn inequality is (1.7) for any $v \in H^1(\Omega)^n$ with

$$(1.8) \quad \int_{\Omega} v \, dx = 0 \quad \text{and} \quad \int_{\Omega} D_{\text{ss}}v \, dx = 0.$$

This is applied to piecewise H^1 vector fields, where (1.8) holds piecewise. Then C_K exclusively depends on n and the shape regularity of the triangulation. A proof of all this is provided in [10]. The set of symmetric matrices is denoted by $\mathbb{S} \equiv \text{sym}(\mathbb{R}^{n \times n})$. Given two vectors $a, b \in \mathbb{R}^n$, recall the vector product $a \otimes b := ab^t \in \mathbb{R}^{n \times n}$. The deviatoric part of $M \in \mathbb{R}^{n \times n}$ is defined by $\text{dev}M := M - \text{tr}(M)\mathbf{I}_{n \times n}/n$ with the trace $\text{tr}(M) := M : \mathbf{I}_{n \times n}$. The notation $A \lesssim B$ means $A \leq CB$ for a generic constant C , $A \approx B$ abbreviates $A \lesssim B$ and $B \lesssim A$.

2. DISCRETE PROBLEM

This section recalls the HHO methodology introduced in [24, 23, 26, 22] for the linear elastic model problem of Subsection 1.2.

2.1. Triangulation. Let \mathcal{T} be a regular triangulation into simplices with the set of sides \mathcal{F} . The set of interior sides (resp. boundary sides) is denoted by $\mathcal{F}(\Omega)$ (resp. $\mathcal{F}(\partial\Omega) := \mathcal{F} \setminus \mathcal{F}(\Omega)$). We assume that the Dirichlet boundary Γ_D can be exactly resolved by the triangulation, i.e., the set $\mathcal{F}_D := \{F \in \mathcal{F} : F \subset \Gamma_D\}$ of Dirichlet sides covers $\Gamma_D = \cup \mathcal{F}_D$. Fix the orientation of the normal vector ν_F of an interior side $F \in \mathcal{F}(\Omega)$ and $\nu_F := \nu|_F$ for any boundary side $F \in \mathcal{F}(\partial\Omega)$. Given $F \in \mathcal{F}(\Omega)$, $T_{\pm} \in \mathcal{T}$ denotes the unique simplex with $F \subset \partial T_{\pm}$ and $\nu_{T_{\pm}}|_F = \pm \nu_F$. The jump $[v]_F$ of any function $v : \Omega \rightarrow \mathbb{R}$ with $v|_{T_{\pm}} \in W^{1,1}(\text{int}(T_{\pm}))$ along $F \in \mathcal{F}(\Omega)$ is defined by $[v]_F := v|_{T_+} - v|_{T_-} \in L^1(F; \mathbb{R}^m)$. If $F \in \mathcal{F}(\partial\Omega)$, then $[v]_F := v|_F$. For any $T \in \mathcal{T}$ (resp. $F \in \mathcal{F}$), define the simplex patch $\Omega(T) := \text{int}(\cup_{K \in \mathcal{T}, K \cap T \neq \emptyset} K)$ (resp. side patch $\omega(F) := \text{int}(\cup_{T \in \mathcal{T}, F \in \mathcal{F}(T)} T)$). The set $H^1(\mathcal{T})$ is the space of all piecewise H^1 function with respect to the triangulation \mathcal{T} . The notation ∇_{pw} denotes the piecewise application of the differential operator ∇ (even without explicit reference to \mathcal{T}). This notation applies to the differential operators div and ε as well. In context of mesh-refining algorithms, there is an initial triangulation \mathcal{T}_0 with the set \mathcal{V}_0 (resp. \mathcal{F}_0) of vertices (resp. sides) of \mathcal{T}_0 . We assume that \mathcal{T}_0 satisfies the initial condition (IC) from [39, Section 4, (a)–(b)] to guarantee that the triangulations generated by successive refinements of \mathcal{T}_0 with the newest-vertex-bisection (NVB) algorithm [35, 39] are shape-regular. The set of all such triangulations is denoted by \mathbb{T} and $\mathcal{T} \in \mathbb{T}$ is understood throughout the remaining parts of this paper.

2.2. Finite element spaces. Given a subset $M \subset \mathbb{R}^n$ of diameter h_M , let $P_k(M)$ denote the space of polynomials on M of total degree at most k . For any $v \in L^1(M)$, $\Pi_M^k v \in P_k(M)$ denotes the L^2 projection of v onto $P_k(M)$. The space of piecewise polynomials of degree at most k with respect to \mathcal{T} (resp. \mathcal{F}) is denoted by $P_k(\mathcal{T})$ (resp. $P_k(\mathcal{F})$). The continuous version of $P_{k+1}(\mathcal{T})^n$ with vanishing boundary data on Γ_D reads $S_D^{k+1}(\mathcal{T}) := P_{k+1}(\mathcal{T})^n \cap V$. Given $v \in L^1(\Omega)$ (resp. $v \in L^1(\cup \mathcal{F})$), the L^2 projection $\Pi_{\mathcal{T}}^k v$ (resp. $\Pi_{\mathcal{F}}^k v$) of v onto $P_k(\mathcal{T})$ (resp. $P_k(\mathcal{F})$) is $(\Pi_{\mathcal{T}}^k v)|_T = \Pi_T^k v|_T$ in $T \in \mathcal{T}$ (resp. $(\Pi_{\mathcal{F}}^k v)|_F = \Pi_F^k v|_F$ along $F \in \mathcal{F}$). The piecewise constant mesh-size function $h_{\mathcal{T}} \in P_0(\mathcal{T})$ reads $h_{\mathcal{T}}|_T = h_T$; $h_{\max} := \max_{T \in \mathcal{T}} h_T$ is the maximal simplex diameter in \mathcal{T} . For any $f \in L^2(\Omega)^n$ and $g \in L^2(\Gamma_N)^n$, define $\text{osc}(f, \mathcal{T}) := \|h_{\mathcal{T}}(1 - \Pi_{\mathcal{T}}^k)f\|$ and $\text{osc}(g, \mathcal{F}_N)^2 := \sum_{F \in \mathcal{F}_N} h_F \|(1 - \Pi_F^k)g\|_{L^2(F)}^2$.

2.3. Discrete spaces. Given a fixed natural number $k \geq 1$, let

$$(2.1) \quad V_h := P_k(\mathcal{T})^n \times P_k(\mathcal{F} \setminus \mathcal{F}_D)^n$$

denote the discrete ansatz space for V . In this definition, $P_k(\mathcal{F} \setminus \mathcal{F}_D)^n$ is a subspace of $P_k(\mathcal{F})^n$ by zero extension: $v_{\mathcal{F}}|_F \equiv 0$ on Dirichlet sides $F \in \mathcal{F}_D$ to model the homogeneous Dirichlet boundary condition of $v_{\mathcal{F}} \in P_k(\mathcal{F} \setminus \mathcal{F}_D)^n$. We note that the HHO method in this paper is *not* well-posed for $k = 0$ and refer to [7] for the lowest-order case. For any $v_h = (v_{\mathcal{T}}, v_{\mathcal{F}}) \in V_h$, we abbreviate $v_T := v_{\mathcal{T}}|_T$ in a simplex $T \in \mathcal{T}$ and $v_F := v_{\mathcal{F}}|_F$ along a side $F \in \mathcal{F}$. A norm in V_h reads

$$(2.2) \quad \|v_h\|_h^2 := \|\varepsilon_{\text{pw}}(v_{\mathcal{T}})\|_{L^2(\Omega)}^2 + \sum_{T \in \mathcal{T}} \sum_{F \in \mathcal{F}(T)} h_F^{-1} \|v_F - v_T\|_{L^2(F)}^2.$$

The interpolation operator $I : V \rightarrow V_h$ maps $v \in V$ to $Iv := (\Pi_{\mathcal{T}}^k v, \Pi_{\mathcal{F}}^k v) \in V_h$.

2.4. Reconstructions and stabilization. The potential reconstruction $\mathcal{R} : V_h \rightarrow P_{k+1}(\mathcal{T})^n$ maps $v_h = (v_{\mathcal{T}}, v_{\mathcal{F}}) \in V_h$ onto $\mathcal{R}v_h \in P_{k+1}(\mathcal{T})^n$ such that

$$(2.3) \quad \begin{aligned} & \int_{\Omega} \varepsilon_{\text{pw}}(\mathcal{R}v_h) : \varepsilon_{\text{pw}}(\varphi_{k+1}) \, dx \\ &= - \int_{\Omega} v_{\mathcal{T}} \cdot \text{div}_{\text{pw}} \varepsilon_{\text{pw}}(\varphi_{k+1}) \, dx + \sum_{F \in \mathcal{F}} \int_F v_F \cdot [\varepsilon_{\text{pw}}(\varphi_{k+1})]_F \nu_F \, ds \end{aligned}$$

for any $\varphi_{k+1} \in P_{k+1}(\mathcal{T})^n$. The system (2.3) of linear equations defines $\mathcal{R}v_h$ uniquely up to the components associated with rigid-body motions. The latter are fixed by

$$(2.4) \quad \int_T \mathcal{R}v_h \, dx = \int_T v_T \, dx \quad \text{and} \quad \int_T D_{ss} \mathcal{R}v_h \, dx = \sum_{F \in \mathcal{F}(T)} \int_F \text{asym}(\nu_T \otimes v_F) \, ds$$

for any $T \in \mathcal{T}$. The gradient reconstruction $\mathcal{G}v_h \in P_k(\mathcal{T})^{n \times n}$ of v_h solves

$$(2.5) \quad \int_{\Omega} \mathcal{G}v_h : \Phi_k \, dx = - \int_{\Omega} v_{\mathcal{T}} \cdot \text{div}_{\text{pw}} \Phi_k \, dx + \sum_{F \in \mathcal{F}} \int_F v_F \cdot [\Phi_k]_F \nu_F \, ds$$

for any $\Phi_k \in P_k(\mathcal{T})^{n \times n}$. The symmetric part of $\mathcal{G}v_h$ is denoted by $\varepsilon_h v_h := \text{sym}(\mathcal{G}v_h) \in P_k(\mathcal{T}; \mathbb{S})$. It is shown in [26, Section 7.2.5] that ε_h coincides with the symmetric gradient reconstruction of v_h from [8], while the trace of $\varepsilon_h v_h$ is the divergence reconstruction of v_h from [23]. With the difference operators

$$(2.6) \quad \delta_T^k v_h := \Pi_T^k(v_T - \mathcal{R}v_h) \in P_k(T)^n \quad \text{and} \quad \delta_{TF}^k v_h := \Pi_F^k(v_F - \mathcal{R}v_h|_T) \in P_k(F)^n$$

for any simplex $T \in \mathcal{T}$ and side $F \in \mathcal{F}(T)$ [26, Section 2.1.4], the local stabilization $s_T(u_h, v_h)$ of $u_h = (u_{\mathcal{T}}, u_{\mathcal{F}})$, $v_h = (v_{\mathcal{T}}, v_{\mathcal{F}}) \in V_h$ from [23, 8] reads

$$(2.7) \quad s_T(u_h, v_h) := \sum_{F \in \mathcal{F}(T)} h_F^{-1} \int_F (\delta_{TF}^k u_h - \delta_T^k u_h) \cdot (\delta_{TF}^k v_h - \delta_T^k v_h) \, ds.$$

The global weighted and non-weighted version of (2.7), namely

$$s(u_h, v_h) := \sum_{T \in \mathcal{T}} \mu|_T s_T(u_h, v_h) \quad \text{and} \quad \widehat{s}(u_h, v_h) := \sum_{T \in \mathcal{T}} s_T(u_h, v_h)$$

for any $u_h, v_h \in V_h$, induce the seminorms $|\bullet|_s := s(\bullet, \bullet)^{1/2}$ and $|\bullet|_{\widehat{s}} := \widehat{s}(\bullet, \bullet)^{1/2}$ on V_h . While the weighted version s with the Lamé parameter $\mu|_T > 0$ (from the isotropic elasticity tensor \mathbb{C}) is utilized in the numerical scheme, \widehat{s} serves only for theoretical purposes. The reconstructions \mathcal{R} , \mathcal{G} , and the stabilization s can be computed simplex-wise and, therefore, in parallel.

2.5. New equivalence of stabilizations. This subsection proves the local equivalence of s and the alternative stabilization \widetilde{s} defined by $\widetilde{s}(u_h, v_h) = \sum_{T \in \mathcal{T}} \widetilde{s}_T(u_h, v_h)$ and

$$(2.8) \quad \widetilde{s}_T(u_h, v_h) := h_T^{-2} (\delta_T^k u_h, \delta_T^k v_h)_{L^2(T)} + \sum_{F \in \mathcal{F}(T)} h_F^{-1} (\delta_{TF}^k u_h, \delta_{TF}^k v_h)_{L^2(F)}$$

for any $T \in \mathcal{T}$ and $u_h, v_h \in V_h$. This stabilization \widetilde{s} was utilized in an HHO method for the Poisson equation in [26], but its equivalence to the classical HHO stabilization from [24] was established later [4, Theorem 4]. Theorem 2.1 below extends the equivalence $s \approx \widetilde{s}$ from [4] to the linear elasticity model problem. We note that Theorem 2.1 holds for general polytopal meshes.

Theorem 2.1 (equivalence of stabilizations). *Any $v_h = (v_{\mathcal{T}}, v_{\mathcal{F}}) \in V_h$ and $T \in \mathcal{T}$ satisfy $s_T(v_h, v_h) \approx \widetilde{s}_T(v_h, v_h)$.*

Proof. The assertion \lesssim follows immediately from the triangle and the discrete trace inequality. The remaining parts of this proof are therefore devoted to the reverse direction \gtrsim . A triangle and a discrete trace inequality imply

$$(2.9) \quad \|\delta_{TF}^k v_h\|_{L^2(F)} \lesssim \|\delta_{TF}^k v_h - \delta_T^k v_h\|_{L^2(F)} + h_T^{-1/2} \|\delta_T^k v_h\|_{L^2(T)}$$

for any $F \in \mathcal{F}(T)$. Therefore, it remains to prove $h_T^{-1} \|\delta_T^k v_h\|_{L^2(T)} \lesssim s_T(u_h, v_h)^{1/2}$. Let x_T denote the midpoint of T . Define the rigid-body motion $\varphi_{\text{RM}} := \Pi_T^0 \delta_T^k v_h +$

$(\Pi_T^0 D_{\text{ss}} \delta_T^k v_h)(x - x_T)$ as in [23]. Since $\Pi_T^0 \delta_T^k v_h = 0$ from (2.4), we infer

$$(2.10) \quad h_T^{-1} \|\varphi_{\text{RM}}\|_{L^2(T)} \approx \|\Pi_T^0 D_{\text{ss}} \delta_T^k v_h\|_{L^2(T)} = |T|^{-1/2} \left| \int_T D_{\text{ss}} \delta_T^k v_h \, dx \right|.$$

The outer normal vector ν_T is constant along any $F \in \mathcal{F}(T)$ and hence, the convention (2.4) in the definition of \mathcal{R} and an integration by parts show

$$\sum_{F \in \mathcal{F}(T)} \int_F \text{asym}(\nu_T \otimes \delta_{TF}^k v_h) \, ds = \sum_{F \in \mathcal{F}(T)} \int_F \text{asym}(\nu_T \otimes (v_F - \mathcal{R}v_h|_T)) \, ds = 0.$$

In combination with another integration by parts, we obtain

$$\begin{aligned} \int_T D_{\text{ss}} \delta_T^k v_h \, dx &= \sum_{F \in \mathcal{F}(T)} \int_F \text{asym}(\nu_T \otimes \delta_T^k v_h) \, ds \\ &= \sum_{F \in \mathcal{F}(T)} \int_F \text{asym}(\nu_T \otimes (\delta_T^k v_h - \delta_{TF}^k v_h)) \, ds. \end{aligned}$$

This, (2.10), and a Cauchy inequality reveal

$$h_T^{-1} \|\varphi_{\text{RM}}\|_{L^2(T)} \lesssim \sum_{F \in \mathcal{F}(T)} h_F^{-1/2} \|\delta_{TF}^k v_h - \delta_T^k v_h\|_{L^2(F)} \lesssim s_T(v_h, v_h)^{1/2}.$$

Since $h_T^{-1} \|\delta_T^k v_h - \varphi_{\text{RM}}\|_{L^2(T)} \lesssim \|\varepsilon(\delta_T^k v_h)\|_{L^2(T)}$ from a Poincaré and the (second) Korn inequality (1.7),

$$(2.11) \quad h_T^{-1} \|\delta_T^k v_h\|_{L^2(T)} \lesssim s_T(v_h, v_h)^{1/2} + \|\varepsilon(\delta_T^k v_h)\|_{L^2(T)}.$$

The proof of $\|\varepsilon(\delta_T^k v_h)\|_{L^2(T)}^2 \lesssim s_T(v_h, v_h)$ below generalizes that of [4, Theorem 4]. An integration by parts provides

$$(2.12) \quad \|\varepsilon(\delta_T^k v_h)\|_{L^2(T)}^2 = -(\delta_T^k v_h, \text{div } \varepsilon(\delta_T^k v_h))_{L^2(T)} + (\delta_T^k v_h, \varepsilon(\delta_T^k v_h) \nu_T)_{L^2(\partial T)}.$$

Since $\text{div } \varepsilon(\delta_T^k v_h) \in P_{k-2}(T)^n \subset P_k(T)^n$ with the convention $P_{-1}(T) = \{0\}$, another integration by parts and the definition (2.3) of \mathcal{R} result in

$$\begin{aligned} -(\Pi_T^k \mathcal{R}v_h, \text{div } \varepsilon(\delta_T^k v_h))_{L^2(T)} &= -(\mathcal{R}v_h, \text{div } \varepsilon(\delta_T^k v_h))_{L^2(T)} \\ &= -(v_T, \text{div } \varepsilon(\delta_T^k v_h))_{L^2(T)} + \sum_{F \in \mathcal{F}(T)} (v_F - \mathcal{R}v_h|_T, \varepsilon(\delta_T^k v_h) \nu_T)_{L^2(F)}. \end{aligned}$$

Recall $\delta_T^k v_h = \Pi_T^k (v_T - \mathcal{R}v_h)$ to rewrite this as

$$(2.13) \quad (\delta_T^k v_h, \text{div } \varepsilon(\delta_T^k v_h))_{L^2(T)} = \sum_{F \in \mathcal{F}(T)} (\delta_{TF}^k v_h, \varepsilon(\delta_T^k v_h) \nu_T)_{L^2(F)}$$

with $\varepsilon(\delta_T^k v_h) \nu_T \in P_k(F)$ along any $F \in \mathcal{F}(T)$ in the last step. The combination of (2.12)–(2.13) with a Cauchy and discrete trace inequality reveals

$$(2.14) \quad \|\varepsilon(\delta_T^k v_h)\|_{L^2(T)}^2 \lesssim \sum_{F \in \mathcal{F}(T)} h_F^{-1/2} \|\delta_{TF}^k v_h - \delta_T^k v_h\|_{L^2(F)} \|\varepsilon(\delta_T^k v_h)\|_{L^2(T)}.$$

Hence, $\|\varepsilon(\delta_T^k v_h)\|_{L^2(T)}^2 \lesssim s_T(v_h, v_h)$, (2.9), and (2.11) conclude the proof. \square

While Theorem 2.1 also holds for general polytopal meshes, it provides a clear description of the kernel of $|\bullet|_s$ on triangulations into simplices. Define the set $\text{CR}_D^{k+1}(\mathcal{T}) := \{v_{k+1} \in P_{k+1}(\mathcal{T})^n : \Pi_F^k [v_{k+1}]_F = 0 \text{ for any } F \in \mathcal{F} \setminus \mathcal{F}_N\}$ of Crouzeix-Raviart functions. The interpolation $\mathbf{I} : V \rightarrow V_h$ can be extended to $\mathbf{I} : V + \text{CR}_D^{k+1}(\mathcal{T}) \rightarrow V_h$ because $\Pi_F^k v_{\text{CR}}$ is uniquely defined for Crouzeix-Raviart functions.

Corollary 2.2 (kernel of $|\bullet|_s$). *Any given $v_h \in V_h$ satisfies $|v_h|_s = 0$ if and only if $v_h = \mathbf{I}v_{\text{CR}}$ holds for some $v_{\text{CR}} \in \text{CR}_D^{k+1}(\mathcal{T})$.*

Proof. If $v_h \in V_h$ with $|v_h|_s = 0$, then Theorem 2.1 implies that $\Pi_{\mathcal{T}}^k \mathcal{R}v_h = v_{\mathcal{T}}$ and $\Pi_F^k \mathcal{R}v_h|_T = v_F$ for any $T \in \mathcal{T}$ and $F \in \mathcal{F}(T)$. This and the convention $v_F \equiv 0$ on $F \in \mathcal{F}_D$ shows $\Pi_F^k [\mathcal{R}v_h]_F = 0$ for any $F \in \mathcal{F} \setminus \mathcal{F}_N$ and so, $\mathcal{R}v_h \in \text{CR}_D^{k+1}(\mathcal{T})$ with $I\mathcal{R}v_h = v_h$. On the other hand, let $v_{\text{CR}} \in \text{CR}_D^{k+1}(\mathcal{T})$ be given. A piecewise integration by parts proves that $v_{\text{CR}} \in P_{k+1}(\mathcal{T})^n$ satisfies (2.3)–(2.4) with $v_{\mathcal{T}} := \Pi_{\mathcal{T}}^k v_{\text{CR}}$ and $v_F := \Pi_F^k v_{\text{CR}}$ for any $F \in \mathcal{F}$, whence

$$(2.15) \quad \mathcal{R}Iv_{\text{CR}} = v_{\text{CR}}.$$

This and Theorem 2.1 conclude the proof of $|Iv_{\text{CR}}|_s = 0$. \square

2.6. Elementary properties. The following results state the characteristic properties of reconstruction operators in the HHO methodology.

Lemma 2.3 (commuting diagram). *Any $v \in V$ and $s \in \mathbb{R}$ satisfy*

$$\Pi_{\mathcal{T}}^k \varepsilon(v) = \varepsilon_h I v \quad \text{and} \quad \Pi_{\mathcal{T}}^k \mathbb{C}^s \varepsilon(v) = \mathbb{C}^s \varepsilon_h I v.$$

Proof. The first identity follows from $\Pi_{\mathcal{T}}^k Dv = \mathcal{G}Iv$ [26, Eq. (4.40)] and is stated in [8, Eq. (18)]. The second identity is an immediate consequence of the first for piecewise constant parameters λ, μ . \square

Lemma 2.4 (best approximation of $\mathcal{R} \circ I$). *Any $v \in V$ satisfies*

$$(2.16) \quad \|D_{\text{pw}}(v - \mathcal{R}Iv)\| \lesssim \|\varepsilon_{\text{pw}}(v - \mathcal{R}Iv)\| = \min_{v_{k+1} \in P_{k+1}(\mathcal{T})^n} \|\varepsilon_{\text{pw}}(v - v_{k+1})\|.$$

Proof. From (2.4), we infer for any $v \in V$ and $T \in \mathcal{T}$ that

$$\int_T (v - \mathcal{R}Iv) \, dx = 0 \quad \text{and} \quad \int_T D_{\text{ss}}(v - \mathcal{R}Iv) \, dx = 0.$$

Hence, the (second) Korn inequality (1.7) proves the inequality in (2.16). The equality in (2.16) follows from the L^2 orthogonality $\varepsilon_{\text{pw}}(v - \mathcal{R}Iv) \perp \varepsilon_{\text{pw}}(P_{k+1}(\mathcal{T})^n)$ [23, Eq. (19)]. \square

A straightforward consequence of Lemma 2.3–2.4 is the following.

Remark 2.5 ($\varepsilon_h \circ I = \varepsilon$ in $S_D^{k+1}(\mathcal{T})$). If $v \in S_D^{k+1}(\mathcal{T})$, then $\varepsilon(v) \in \varepsilon(P_{k+1}(\mathcal{T})^n) \subset P_k(\mathcal{T})^{n \times n}$. Lemma 2.3–2.4 imply $\varepsilon(v) = \varepsilon_h I v = \varepsilon_{\text{pw}}(\mathcal{R}Iv)$.

Another implication of Theorem 2.1 is the following bound.

Lemma 2.6 ($\varepsilon_{\text{pw}} \circ \mathcal{R}$ vs ε_h). *Any $v_h \in V_h$ and $T \in \mathcal{T}$ satisfy*

$$\|\varepsilon(\mathcal{R}v_h) - \varepsilon_h v_h\|_{L^2(T)}^2 \lesssim s_T(v_h, v_h).$$

Proof. Given $v_h = (v_{\mathcal{T}}, v_{\mathcal{F}}) \in V_h$, abbreviate $\Phi_k := (\varepsilon_{\text{pw}}(\mathcal{R}v_h) - \varepsilon_h v_h)|_T \in P_k(T; \mathbb{S})$. The definition of ε_h in (2.5) and an integration by parts imply

$$\begin{aligned} \|\Phi_k\|_{L^2(T)}^2 &= (\varepsilon(\mathcal{R}v_h) - \varepsilon_h v_h, \Phi_k)_{L^2(T)} \\ &= (v_T - \mathcal{R}v_h, \text{div } \Phi_k)_{L^2(T)} + \sum_{F \in \mathcal{F}(T)} (\mathcal{R}v_h|_T - v_F, \Phi_k \nu_F)_{L^2(F)}. \end{aligned}$$

Since $\text{div } \Phi_k \in P_k(T)^n$ and $\Phi_k \nu_F \in P_k(F)^n$, this, a Cauchy inequality, the inverse inequality $\|\text{div } \Phi_k\|_{L^2(T)} \lesssim h_T^{-1} \|\Phi_k\|_{L^2(T)}$, and the discrete trace inequality $\|\Phi_k\|_{L^2(F)} \lesssim h_F^{-1/2} \|\Phi_k\|_{L^2(T)}$ for any $F \in \mathcal{F}(T)$ provide

$$\|\Phi_k\|_{L^2(T)}^2 \lesssim \|h_T^{-1} \delta_T^k v_h\|_{L^2(T)}^2 + \sum_{F \in \mathcal{F}(T)} h_F^{-1} \|\delta_{TF}^k v_h\|_{L^2(F)}^2 = \tilde{s}_T(v_h, v_h).$$

This and Theorem 2.1 conclude the proof. \square

2.7. Discrete formulation. The discrete problem seeks the solution $u_h \in V_h$ to

$$(2.17) \quad a_h(u_h, v_h) = \int_{\Omega} f \cdot v_{\mathcal{T}} dx + \int_{\Gamma_N} g \cdot v_{\mathcal{F}} ds \quad \text{for all } v_h = (v_{\mathcal{T}}, v_{\mathcal{F}}) \in V_h$$

with the discrete bilinear form

$$(2.18) \quad a_h(u_h, v_h) := (\mathbb{C}\varepsilon_h u_h, \varepsilon_h v_h)_{L^2(\Omega)} + s(u_h, v_h).$$

The following result proves that a_h is a scalar product in V_h and the induced norm is denoted by $\|\bullet\|_{a_h}$. Recall the norm $\|\bullet\|_h$ from (2.2).

Theorem 2.7 (Existence and uniqueness of discrete solutions). *There exist positive constants C_1, C_2 that solely depend on k and the shape regularity of \mathcal{T} with*

$$(2.19) \quad C_1^{-1} \|v_h\|_h \leq \|\varepsilon_h v_h\| + |v_h|_{\tilde{s}} \approx \|\varepsilon_{\text{pw}}(\mathcal{R}v_h)\| + |v_h|_{\tilde{s}} \leq C_2 \|v_h\|_h$$

for any $v_h \in V_h$. In particular, a_h from (2.18) is a scalar product on V_h and there exists a unique discrete solution to (2.17).

Proof. This result is established in [26, Section 7.2.6]. \square

Throughout the remaining parts of this paper, u_h denotes the unique solution to the discrete problem (2.17) and $\sigma_h := \mathbb{C}\varepsilon_h u_h \in P_k(\mathcal{T}; \mathbb{S})$ is the discrete stress.

2.8. Comments on alternative schemes.

Remark 2.8 (equivalent stabilization). The results of this paper can be extended to (2.17) with s replaced by \tilde{s} (by equivalence of stabilizations in Theorem 2.1).

Remark 2.9 (HDG stabilization). Another HHO method utilizes the ansatz space $V_h := P_{k+1}(\mathcal{T})^n \times P_k(\mathcal{F} \setminus \mathcal{F}_D)^n$ with the Lehrenfeld-Schöberl stabilization

$$(2.20) \quad s_T^{\text{HDG}}(u_h, v_h) := \sum_{F \in \mathcal{F}(T)} h_F^{-1} \int_F \Pi_F^k(u_F - u_T) \cdot \Pi_F^k(v_F - v_T) ds$$

for $T \in \mathcal{T}$ from the HDG methodology [34]. Straight-forward adaptations of the arguments in the proof of Theorem 2.1 provides the local equivalence

$$(2.21) \quad s_T^{\text{HDG}}(v_h, v_h)^{1/2} \approx h_T^{-1} \|\delta_T^{(k+1)} v_h\|_{L^2(T)} + \sum_{F \in \mathcal{F}(T)} h_F^{-1/2} \|\delta_{TF}^k v_h\|_{L^2(F)}.$$

This holds for any $v_h \in P_{k+1}(\mathcal{T})^n \times P_k(\mathcal{F} \setminus \mathcal{F}_D)^n$ and the modified difference operator $\delta_T^{(k+1)} v_h := v_T - \mathcal{R}v_h \in P_{k+1}(T)^n$ and $\delta_{TF}^k v_h$ from (2.6) with the representation $\Pi_F^k(v_F - v_T) = \Pi_F^k(\delta_{TF}^k v_h - \delta_T^{(k+1)} v_h)$ from [26, Section 5.1.6].

Remark 2.10 (HDG error control). The equivalence (2.21) allow for a generalization of the error analysis of this paper to the HHO scheme from [26, Section 5.1.6], which can also be seen as an HDG method. In particular, the error estimates (1.3)–(1.4) hold verbatim with the discrete ansatz space $V_h = P_{k+1}(\mathcal{T})^n \times P_k(\mathcal{F} \setminus \mathcal{F}_D)^n$ and the stabilization s^{HDG} from (2.20).

Remark 2.11 (Comparison to conforming, nonconforming, and mixed FEM). An adaptive conforming hp FEM is preferable if high accuracy is mandatory. For lower-order approximations, the analyzed scheme is one of the simplest λ -robust methods in 3D. (Notice that the nonconforming Kouhia-Stenberg FEM [31] applies only in 2D). The Arnold-Winther mixed scheme [2] is more elaborate than the locking-free conforming FEM for $k \geq 4$ [3]. For weakly symmetric FEM, we refer to [33] and the references quoted therein, but mention that strong symmetry is often desirable.

Remark 2.12 (Comparison within skeletal methods). The simplest VEM method for $k = 1$ is not looking-free [42]. Compared to discontinuous Galerkin schemes, the HHO methodology is parameter-free. A close competitor is the HDG method with the Lehrenfeld-Schöberl stabilization from [34], cf. Remark 2.9–2.10.

Remark 2.13 (Stokes equation). The incompressible limit as $\lambda \rightarrow \infty$ leads formally to the Stokes equations in the symmetric formulation (i.e. in terms of the linear Green strain ε). The estimates in this paper are λ -robust and hence hold for the resulting Stokes problem as well and lead to a stable novel HHO discretisation with corresponding error terms (1.3)–(1.4). A similar extension is also expected for the known HHO scheme [25] and their HDG relatives in the non-symmetric form from the textbooks [30, 11, 6] (when $\Gamma_N = \emptyset$, the linear Green strain ε can be replaced by the gradient D).

3. A PRIORI ERROR ANALYSIS

This section establishes the quasi-best approximation result (1.3).

3.1. Main result. Let $u \in V$ denote the exact solution to (1.2) and $\sigma = \mathbb{C}\varepsilon(u)$. To obtain λ -robust error estimates for the L^2 stress error $\|\sigma - \sigma_h\|$, the tr-dev-div lemma stated in Lemma 3.7 below is utilized under the following assumption, which imposes mild geometric assumptions on the initial triangulation \mathcal{T}_0 for $|\Gamma_N| > 0$.

Assumption A. Either $|\Gamma_N| = 0$ or there exists $\varphi_0 \in S_D^k(\mathcal{T}_0)$ with $\int_\Omega \operatorname{div} \varphi_0 \, dx \neq 0$.

Remark 3.1 ((A) for $k < n$). Suppose that z is a vertex of \mathcal{T}_0 in the relative interior of Γ_N , define $\varphi_0 := a\varphi_z \in S_D^1(\mathcal{T}_0)$ with a vector $a \in \mathbb{R}^n$ and the nodal basis function φ_z associated with z . Let $\mathcal{F}_z := \{F \in \mathcal{F}_0 : z \in F\} \subset \mathcal{F}_{0,N}$ denote the set of all sides containing z , where $\mathcal{F}_{0,N}$ is the set of Neumann sides of \mathcal{T}_0 . An integration by parts reveals

$$(3.1) \quad n \int_\Omega \operatorname{div} \varphi_0 \, dx = a \cdot \sum_{F \in \mathcal{F}_z} |F| \nu_F.$$

In 2D, there are $|\mathcal{F}_z| = 2$ edges and $a := \sum_{F \in \mathcal{F}_z} |F| \nu_F \neq 0$ leads in (3.1) to (A). In 3D, the same arguments lead to (3.1) for a vertex z in a flat part of Γ_N or z is a convex/concave corner point. Notice that this can always be generated by mesh-refinements.

Remark 3.2 ((A) for $k \geq n$). Given $F \in \mathcal{F}_{0,N}$, consider the face bubble function $b_F := \prod_{z \in \mathcal{V}_0(F)} \varphi_z$ with the set $\mathcal{V}_0(F)$ of all vertices of F . For $\varphi_0 := b_F \nu_F \in S_D^n(\mathcal{T}_0)$, an integration by parts provides

$$\int_\Omega \operatorname{div} \varphi_0 \, dx = \int_F b_F \, dx > 0.$$

In other words, $k \geq n$ implies (A) without any additional geometric assumption.

The following result implies the convergence rates from [23, 26].

Theorem 3.3 (quasi-best approximation). *Suppose (A), then the discrete solution u_h to (2.17) and $\sigma_h = \mathbb{C}\varepsilon_h u_h$ satisfy (1.3). The λ -independent constant C_{qb} exclusively depends on k, Γ_D, Σ_0 , and \mathbb{T} , where*

$$(3.2) \quad \Sigma_0 := \begin{cases} \{\tau \in L^2(\Omega)^{n \times n} : \int_\Omega \operatorname{tr} \tau \, dx = 0\} & \text{if } \Gamma_N = \emptyset \text{ and else} \\ \{\tau \in L^2(\Omega)^{n \times n} : (\tau, \varepsilon(\varphi_0))_{L^2(\Omega)} = 0\} \end{cases}$$

is a closed subspace of $L^2(\Omega)^{n \times n}$ with \mathcal{T}_0 and φ_0 from (A).

Several preliminary results precede the proof of Theorem 3.3 in Subsection 3.5.

3.2. Right inverse. This subsection recalls the right inverse \mathcal{J} of \mathbf{I} from [29]. Let $\mathcal{A} : V_h \rightarrow S_D^{k+1}(\mathcal{T})$ denote the averaging operator that maps $v_h \in V_h$ onto $\mathcal{A}v_h \in S_D^{k+1}(\mathcal{T})$ by averaging all possible values of $\mathcal{R}v_h$ at the nodal degrees of freedom of $S_D^{k+1}(\mathcal{T})$.

Lemma 3.4 (right-inverse). *There exists a linear operator $\mathcal{J} : V_h \rightarrow V$ such that $\mathbf{I} \circ \mathcal{J} = \text{Id}$ and any $v_h \in V_h$ satisfies (a) $\|\varepsilon_{\text{pw}}(\mathcal{J}v_h - \mathcal{R}v_h)\| \lesssim \inf_{v \in V} \|\mathbf{D}_{\text{pw}}(v - \mathcal{R}v_h)\| + |v_h|_{\mathfrak{S}}$ and (b) $\mu_0^{1/2} \|\varepsilon(\mathcal{J}v_h)\| \lesssim \|v_h\|_{a_h}$.*

Proof of Lemma 3.4.a. The construction of \mathcal{J} is provided in [29] for the scalar case with homogeneous boundary condition along the entire body. The extension to the vector-valued case by component-wise application of the operator therein is straightforward with a minor modification in [29, Def. (4.19)] owing to possible Neumann boundary conditions: The set of interior sides $\mathcal{F}(\Omega)$ is replaced by $\mathcal{F} \setminus \mathcal{F}_N$ to enforce homogeneous boundary data only on Γ_D . The estimate

$$(3.3) \quad \|\mathbf{D}_{\text{pw}}(\mathcal{R}v_h - \mathcal{J}v_h)\|^2 \lesssim \sum_{F \in \mathcal{F} \setminus \mathcal{F}_N} h_F^{-1} \|[\mathcal{R}v_h]_F\|_{L^2(F)}^2 + \tilde{\mathfrak{s}}(v_h, v_h)$$

follows from the arguments in the proof of [29, Proposition 4.7], where [29, Proposition 4.6] applies to $(\Pi_{\mathcal{T}}^k(v_{\mathcal{T}} - \mathcal{A}v_h), (\Pi_F^k(v_F - \mathcal{A}v_h))_{F \in \mathcal{F} \setminus \mathcal{F}_D})$ instead of $(v_{\mathcal{T}} - \mathcal{A}v_h, (v_F - \mathcal{A}v_h)_{F \in \mathcal{F} \setminus \mathcal{F}_D})$ in the ultimate formula of [29, p. 2179]. A triangle and a Poincaré inequality along $F \in \mathcal{F}$ imply

$$(3.4) \quad \|[\mathcal{R}v_h]_F\|_{L^2(F)} \lesssim h_F \|\mathbf{D}_{\text{pw}} \mathcal{R}v_h \times \nu_F\|_{L^2(F)} + \|[\Pi_F^0 \mathcal{R}v_h]_F\|_{L^2(F)}.$$

The bubble-function techniques [44] lead to the efficiency estimate

$$(3.5) \quad h_F^{1/2} \|\mathbf{D}_{\text{pw}} \mathcal{R}v_h \times \nu_F\|_{L^2(F)} \lesssim \inf_{v \in V} \|\mathbf{D}_{\text{pw}}(v - \mathcal{R}v_h)\|_{L^2(\omega(F))},$$

cf. [4, Lemma 7] for further details. The stability of the L^2 projection and a triangle inequality reveal

$$\|[\Pi_F^0 \mathcal{R}v_h]_F\|_{L^2(F)} \leq \|[\Pi_F^k \mathcal{R}v_h]_F\|_{L^2(F)} \leq \sum_{\{T \in \mathcal{T} : F \in \mathcal{F}(T)\}} \|\Pi_F^k(v_F - \mathcal{R}v_h|_T)\|_{L^2(F)}.$$

The combination of this with (3.3)–(3.5) results in

$$\|\mathbf{D}_{\text{pw}}(\mathcal{R}v_h - \mathcal{J}v_h)\|^2 \lesssim \inf_{v \in V} \|\mathbf{D}_{\text{pw}}(v - \mathcal{R}v_h)\|^2 + \tilde{\mathfrak{s}}(v_h, v_h).$$

This, Theorem 2.1, and $\|\varepsilon_{\text{pw}}(\mathcal{R}v_h - \mathcal{J}v_h)\| \leq \|\mathbf{D}_{\text{pw}}(\mathcal{R}v_h - \mathcal{J}v_h)\|$ prove (a).

Proof of Lemma 3.4.b. Recall the norm $\|\bullet\|_h$ from (2.2). Given $F \in \mathcal{F}$, the triangle inequality provides $\|[\mathcal{R}v_h]_F\|_{L^2(F)} \leq \|[\mathcal{R}v_h - v_{\mathcal{T}}]_F\|_{L^2(F)} + \|[v_{\mathcal{T}}]_F\|_{L^2(F)}$ and $\|[v_{\mathcal{T}}]_F\|_{L^2(F)} \leq \sum_{\{T \in \mathcal{T} : F \in \mathcal{F}(T)\}} \|v_T - v_F\|_{L^2(T)}$. This, (3.3), and a discrete trace inequality lead to

$$\|\mathbf{D}_{\text{pw}}(\mathcal{R}v_h - \mathcal{J}v_h)\| \lesssim \|h_{\mathcal{T}}^{-1}(\mathcal{R}v_h - v_{\mathcal{T}})\|_{L^2(\Omega)} + \tilde{\mathfrak{s}}(v_h, v_h)^{1/2} + \|v_h\|_h.$$

In combination with $\|h_{\mathcal{T}}^{-1}(\mathcal{R}v_h - \Pi_{\mathcal{T}}^k \mathcal{R}v_h)\|_{L^2(\Omega)} \lesssim \|\varepsilon_{\text{pw}}(\mathcal{R}v_h)\|$ from [23, p. 8] and a triangle inequality, we infer

$$(3.6) \quad \|\mathbf{D}_{\text{pw}}(\mathcal{R}v_h - \mathcal{J}v_h)\| \lesssim \|\varepsilon_{\text{pw}}(\mathcal{R}v_h)\| + \tilde{\mathfrak{s}}(v_h, v_h)^{1/2} + \|v_h\|_h.$$

Theorem 2.1 and 2.7 imply $\|\varepsilon_{\text{pw}}(\mathcal{R}v_h)\| + \tilde{\mathfrak{s}}(v_h, v_h)^{1/2} + \|v_h\|_h \approx \|\varepsilon_h v_h\| + |v_h|_{\mathfrak{S}}$. This, $\mu_0^{1/2}(\|\varepsilon_h v_h\| + |v_h|_{\mathfrak{S}}) \lesssim \|v_h\|_{a_h}$ by the definition of a_h in (2.18), (3.6), and finally $\|\varepsilon_{\text{pw}}(\mathcal{R}v_h - \mathcal{J}v_h)\| \leq \|\mathbf{D}_{\text{pw}}(\mathcal{R}v_h - \mathcal{J}v_h)\|$ conclude the proof. \square

Remark 3.5 ($\varepsilon_h = \Pi_{\mathcal{T}}^k \circ \varepsilon \circ \mathcal{J}$). The interplay of Lemma 2.3 and the right-inverse \mathcal{J} of \mathbf{I} leads, for any $v_h \in V_h$, to $\Pi_{\mathcal{T}}^k \varepsilon(\mathcal{J}v_h) = \varepsilon_h \mathbf{I} \mathcal{J}v_h = \varepsilon_h v_h$.

3.3. Quasi-best approximation of stabilization. The quasi best-approximation $\|Iv\|_s \lesssim \|\mu^{1/2}\varepsilon_{\text{pw}}(v - \mathcal{R}Iv)\|$ is well-known in the literature [23, 29]. Since the right-hand side of (1.3) involves the L^2 projection, the following result is required. Recall the set \mathbb{T} of admissible triangulations from Subsection 2.1.

Lemma 3.6 (quasi-best approximation of Galerkin projection). *There exist constants C_3, C_4, C_5 , that exclusively depend on k and \mathbb{T} , such that (a)–(b) hold.*

(a) Any $v \in H^1(T)^n$ on $T \in \mathcal{T}$ with $\mathcal{T} \in \mathbb{T}$ satisfies

$$(3.7) \quad C_3^{-1} s_T(Iv, Iv)^{1/2} \leq \|\varepsilon(v - \mathcal{R}Iv)\|_{L^2(T)} \leq C_4 \|(1 - \Pi_T^k)\varepsilon(v)\|_{L^2(T)}.$$

(b) Any $v \in V$ satisfies

$$(3.8) \quad \|\varepsilon(v - \mathcal{J}Iv)\| \leq C_5 \|(1 - \Pi_{\mathcal{T}}^k)\varepsilon(v)\|_{L^2(\Omega)}.$$

Proof of Lemma 3.6.a. Since the first inequality is well-established, the focus is on the second one, which is an extension of the stability estimate in [21, Theorem 3.1]. The arguments therein are sketched below for completeness. Let

$$H^1(T)^n / \text{RM} := \{w \in H^1(T)^n : \int_T w \, dx = 0 \text{ and } \int_T D_{\text{ss}} w \, dx = 0\}.$$

We define the Banach spaces $X := \{v \in H^1(T)^n / \text{RM} : v \perp P_{k+1}(T)^n\}$ endowed with the scalar product $(\varepsilon \bullet, \varepsilon \bullet)_{L^2(T)}$; $Y := L^2(T; \mathbb{S})$ and $Z := P_k(T; \mathbb{S})$ endowed with the L^2 scalar product. Observe, for any $v \in H^1(T)^n$, that $\tilde{v} := v - \mathcal{R}Iv \in X$ from the convention (2.4) and (2.16). Since $(1 - \Pi_T^k)\varepsilon(\tilde{v}) = (1 - \Pi_T^k)\varepsilon(v)$ from $\varepsilon(P_{k+1}(T)^n) \subset P_k(T; \mathbb{S})$, it suffices to show

$$(3.9) \quad \|\varepsilon(v)\|_{L^2(T)} \leq C_{\text{stab}}(T) \|(1 - \Pi_T^k)\varepsilon(v)\|_{L^2(T)} \quad \text{for any } v \in X$$

with a positive constant $C_{\text{stab}}(T) > 0$. The operators $A := (1 - \Pi_T^k)\varepsilon : X \rightarrow Y$ and $B := \Pi_T^k \varepsilon : X \rightarrow Z$ are linear and bounded. If $Av = 0$, then $\varepsilon(v) \in Z$. From [9, Eq. (3.16) in Chapter VI], we infer that D^2v is a tensor-valued polynomial of degree at most $k-1$. Consequently, $v \in P_{k+1}(T)^n$, but the orthogonality $v \perp P_{k+1}(T)^n$ in X reveals $v = 0$. This implies the injectivity of A . Since Z is a finite dimensional space, B is a compact operator. The Pythagoras theorem provides

$$\|v\|_X^2 = \|\varepsilon(v)\|_{L^2(T)}^2 \leq \|(1 - \Pi_T^k)\varepsilon(v)\|_{L^2(T)}^2 + \|\Pi_T^k \varepsilon(v)\|_{L^2(T)}^2 = \|Av\|_Y^2 + \|Bv\|_Z^2.$$

Therefore, the Peetre–Tartar theorem [30, Theorem 2.1] leads to (3.9) with a constant $C_{\text{stab}}(T)$ that may depend on T and k . It remains to prove that $C_{\text{stab}}(T)$ is uniformly bounded for all $T \in \cup \mathbb{T}$. We recall that a congruent mapping Φ is of the form $\Phi(x) = \alpha(Ax + b)$ with a positive number $\alpha > 0$, a vector $b \in \mathbb{R}^n$, and an orthonormal matrix A . It is well known [35, 39] that the number of congruent classes in \mathbb{T} is finite, i.e., there is a finite subset \mathcal{M} of $\cup \mathbb{T}$ such that any $T \in \cup \mathbb{T}$ can be written as $T = \Phi(K)$ with some $K \in \mathcal{M}$ and congruent mapping Φ . Theorem 4.1 from [35] shows that there exist finitely many (one-dimensional) lines through zero such that, given any simplex $T \in \mathbb{T}$ with ordered vertices x_0, \dots, x_n , the edges $x_1 - x_0, x_2 - x_0, \dots, x_n - x_0$ of T lie on these lines. As a conclusion, it is possible to select finite many orthonormal matrices A_1, \dots, A_J (rotations and reflections) such that any $T \in \cup \mathbb{T}$ satisfies $T = \Phi(K)$ for some $K \in \mathcal{M}$ with a congruent mapping $\Phi(x) = \alpha(A_j x + b)$ for some $\alpha > 0$, $b \in \mathbb{R}^n$, and $1 \leq j \leq J$. Set $\mathcal{S} := \cup_{1 \leq j \leq J} A_j \mathcal{M}$, then any admissible simplex $T \in \cup \mathbb{T}$ is the image of some $K \in \mathcal{S}$ under translation and resizing. Notice that the constant $C_{\text{stab}}(T)$ in (3.9) is invariant under these mappings. Since \mathcal{S} is finite, $C_{\text{stab}} := \max_{T \in \mathcal{S}} C_{\text{stab}}(T)$ is a uniform upper bound. \square

Proof of Lemma 3.6.b. In view of (3.7), it remains to prove

$$(3.10) \quad \|\varepsilon_{\text{pw}}(\mathcal{J}Iv - \mathcal{R}Iv)\| \lesssim \|(1 - \Pi_{\mathcal{T}}^k)\varepsilon(v)\|$$

thanks to a triangle inequality. Lemma 3.4 with $v_h = \mathbf{I}v$ and Lemma 2.4 provide

$$\|\varepsilon_{\text{pw}}(\mathcal{J}\mathbf{I}v - \mathcal{R}\mathbf{I}v)\| \lesssim \|\mathbf{D}_{\text{pw}}(v - \mathcal{R}\mathbf{I}v)\| + |\mathbf{I}v|_{\mathfrak{S}} \lesssim \|\varepsilon_{\text{pw}}(v - \mathcal{R}\mathbf{I}v)\| + |\mathbf{I}v|_{\mathfrak{S}}.$$

The combination of this with (3.7) concludes the proof of (3.8). \square

3.4. tr-dev-div lemma. We state a general version of the tr-dev-div lemma.

Lemma 3.7 (tr-dev-div). *Suppose (A), then (a)–(d) hold.*

- (a) *The subspace Σ_0 does not contain the identity matrix $\mathbf{I}_{n \times n} \notin \Sigma_0$.*
- (b) *Given $0 \leq s \leq 1$, any $\tau \in \Sigma_0$ satisfies*

$$(3.11) \quad C_{\text{td}}^{-1} \|\text{tr } \tau\|_{H^s(\Omega)} \leq \|\text{dev } \tau\|_{H^s(\Omega)} + \|\text{div } \tau\|_{H^{s-1}(\Omega)}.$$

The constant C_{td} exclusively depends on Σ_0 and s . In particular,

$$(3.12) \quad \|\tau\|^2 \lesssim \|\mu^{1/2}\tau\|_{\mathbb{C}^{-1}}^2 + \|\text{div } \tau\|_{-1}^2.$$

- (c) *$\sigma - \sigma_h \in \Sigma_0$.*
- (d) *If $\psi \in V$ solves $(\varepsilon(\psi), \varepsilon(\varphi))_{\mathbb{C}} = (\sigma - \sigma_h, \varepsilon(\varphi))_{L^2(\Omega)}$ for any $\varphi \in V$, then $\mathbb{C}\varepsilon(\psi) \in \Sigma_0$.*

Proof of Lemma 3.7.a. The case $|\Gamma_{\text{N}}| = 0$ is trivial. If $|\Gamma_{\text{N}}| > 0$, then the function $\varphi_0 \in S_{\text{D}}^k(\mathcal{T}_0)$ from (A) satisfies $\int_{\Omega} \mathbf{I}_{n \times n} : \varepsilon(\varphi_k) \, dx = \int_{\Omega} \text{div } \varphi_k \, dx \neq 0$. Hence, $\mathbf{I}_{n \times n} \notin \Sigma_0$.

Proof of Lemma 3.7.b. There are several variants of the tr-dev-div lemma known in the literature for $s = 0$, e.g., [6, Proposition 9.1.1]. This version (3.11) with fractional-order Sobolev norms is recently established in [20, Theorem 1]. The bound (3.12) follows from (3.11) with $s = 0$ and the algebraic inequality $|\tau|^2 = |\text{dev } \tau|^2 + |\text{tr } \tau|^2/n \leq 2\mu|\mathbb{C}^{-1/2}\tau|^2 + |\text{tr } \tau|^2/n$ pointwise a.e. in Ω .

Proof of Lemma 3.7.c. Let $|\Gamma_{\text{N}}| = 0$. Recall that λ and μ are constant. The choice $\Phi_k := \mathbf{I}_{n \times n}$ in (2.5) and $u_{\mathcal{F}} = 0$ along $\Gamma_{\text{D}} = \partial\Omega$ provide

$$(\varepsilon_h u_h, \mathbf{I}_{n \times n})_{L^2(\Omega)} = \sum_{F \in \mathcal{F}(\partial\Omega)} \int_F u_F \cdot \nu_F \, ds = 0.$$

This and an integration by parts show

$$(3.13) \quad \begin{aligned} (2\mu + \lambda)^{-1} \int_{\Omega} \text{tr}(\sigma - \sigma_h) \, dx &= \int_{\Omega} \text{div } u \, dx - (\varepsilon_h u_h, \mathbf{I}_{n \times n})_{L^2(\Omega)} \\ &= \int_{\Gamma_{\text{D}}} (u - u_{\mathcal{F}}) \cdot \nu \, ds = 0, \end{aligned}$$

whence $\sigma - \sigma_h \in \Sigma_0$. Consider the case $|\Gamma_{\text{N}}| > 0$. Recall $s(u_h, \mathbf{I}\varphi_0) = 0$ from Corollary 2.2 and $\varepsilon_h \mathbf{I}\varphi_0 = \varepsilon(\varphi_0)$ from Remark 2.5 with $\varphi_0 \in S_{\text{D}}^k(\mathcal{T}_0) \subset S_{\text{D}}^k(\mathcal{T})$ from (A). The variational formulations (1.2) and (2.17) provide

$$(3.14) \quad (\sigma - \sigma_h, \varepsilon(\varphi_0))_{L^2(\Omega)} = (\sigma, \varepsilon(\varphi_0))_{L^2(\Omega)} - (\sigma_h, \varepsilon_h \mathbf{I}\varphi_0)_{L^2(\Omega)} = 0.$$

Proof of Lemma 3.7.d. If $|\Gamma_{\text{N}}| = 0$, then $\int_{\Omega} \text{tr } \mathbb{C}\varepsilon(\psi) \, dx = (2\mu + \lambda) \int_{\Omega} \text{div } \psi \, dx = 0$ from an integration by parts formula. If $|\Gamma_{\text{N}}| > 0$, then the L^2 orthogonality $\mathbb{C}\varepsilon(\psi) \perp \varepsilon(S_{\text{D}}^k(\mathcal{T}))$ by design of ψ and $\sigma - \sigma_h \in \Sigma_0$ from (c) show $\mathbb{C}\varepsilon(\psi) \in \Sigma_0$. \square

We note that $\|\text{div}(\sigma - \sigma_h)\|_{-1}$ arising in Lemma 3.7.b can be bounded as follows.

Lemma 3.8 (bound $\|\text{div}(\sigma - \sigma_h)\|_{-1}$). *The discrete stress σ_h satisfies*

$$\|\text{div}(\sigma - \sigma_h)\|_{-1} \lesssim \text{osc}(f, \mathcal{T}) + \mu_1^{1/2} |u_h|_s.$$

Proof. Given any $\varphi \in V$, Lemma 2.3 and (2.17) imply

$$(\sigma_h, \varepsilon(\varphi))_{L^2(\Omega)} = (\sigma_h, \varepsilon_h \mathbf{I}\varphi)_{L^2(\Omega)} = (f, \Pi_{\mathcal{T}}^k \varphi)_{L^2(\Omega)} + (g, \Pi_{\mathcal{F}}^k \varphi)_{L^2(\Gamma_N)} - s(u_h, \mathbf{I}\varphi).$$

This and the variational formulation (1.2) provide

$$(3.15) \quad \begin{aligned} (\sigma - \sigma_h, \varepsilon(\varphi))_{L^2(\Omega)} &= (f, (1 - \Pi_{\mathcal{T}}^k) \varphi)_{L^2(\Omega)} \\ &+ (g, (1 - \Pi_{\mathcal{F}}^k) \varphi)_{L^2(\Gamma_N)} + s(u_h, \mathbf{I}\varphi). \end{aligned}$$

Standard arguments with Cauchy and Poincaré inequalities lead to

$$(3.16) \quad (\sigma - \sigma_h, \varepsilon(\varphi))_{L^2(\Omega)} \lesssim \text{osc}(f, \mathcal{T}) \|\mathbf{D}\varphi\| + |u_h|_s |\mathbf{I}\varphi|_s$$

for any $\varphi \in H_0^1(\Omega)^n$. Since $|\mathbf{I}\varphi|_s \lesssim \mu_1^{1/2} \|\varepsilon(\varphi)\| \leq \mu_1^{1/2} \|\mathbf{D}\varphi\|$ from (3.7), this and the definition (1.6) of $\|\bullet\|_{-1}$ conclude the assertion. \square

3.5. Proof of Theorem 3.3. The proof is divided into two parts. The first part establishes the quasi-best approximation estimate

$$(3.17) \quad \|e_h\|_{a_h} + |u_h|_s \lesssim \mu_0^{-1/2} (\|(1 - \Pi_{\mathcal{T}}^k) \sigma\| + \text{osc}(f, \mathcal{T}) + \text{osc}(g, \mathcal{F}_N))$$

for the discrete error $\|e_h\|_{a_h}$ with the abbreviation $e_h = (e_{\mathcal{T}}, e_{\mathcal{F}}) := \mathbf{I}u - u_h \in V_h$, while the second part controls the L^2 error of $\sigma - \sigma_h$, namely

$$(3.18) \quad \|\sigma - \sigma_h\| \lesssim (\mu_1/\mu_0)^{1/2} (\|(1 - \Pi_{\mathcal{T}}^k) \sigma\| + \text{osc}(f, \mathcal{T}) + \text{osc}(g, \mathcal{F}_N)).$$

3.5.1. Proof of (3.17). From the identity $-2s(u_h, e_h) = |e_h|_s^2 + |u_h|_s^2 - |\mathbf{I}u|_s^2$, we deduce that

$$(3.19) \quad \begin{aligned} \|\varepsilon_h e_h\|_{\mathbb{C}}^2 + (|e_h|_s^2 + |u_h|_s^2 - |\mathbf{I}u|_s^2)/2 \\ = \|e_h\|_{a_h}^2 - s(\mathbf{I}u, e_h) = (\varepsilon_h \mathbf{I}u, \varepsilon_h e_h)_{\mathbb{C}} - a_h(u_h, e_h). \end{aligned}$$

The formula $\mathbf{I} \circ \mathcal{J} = \text{Id}$ from Lemma 3.4 provides $(\varepsilon_h \mathbf{I}u, \varepsilon_h e_h)_{\mathbb{C}} = (\varepsilon_h \mathbf{I}u, \varepsilon(\mathcal{J}e_h))_{\mathbb{C}}$. This, $\sigma = \mathbb{C}\varepsilon(u)$, and $\Pi_{\mathcal{T}}^k \sigma = \mathbb{C}\varepsilon_h \mathbf{I}u$ from Lemma 2.3 imply

$$(3.20) \quad (\varepsilon_h \mathbf{I}u, \varepsilon_h e_h)_{\mathbb{C}} = (\sigma, \varepsilon(\mathcal{J}e_h))_{L^2(\Omega)} - ((1 - \Pi_{\mathcal{T}}^k) \sigma, \varepsilon(\mathcal{J}e_h))_{L^2(\Omega)}.$$

Observe $(\sigma_h, \varepsilon_h e_h)_{L^2(\Omega)} = (\sigma_h, \varepsilon(\mathcal{J}e_h))_{L^2(\Omega)}$ from Remark 3.5 to verify

$$(\sigma, \varepsilon(\mathcal{J}e_h))_{L^2(\Omega)} - a_h(u_h, e_h) = (\sigma - \sigma_h, \varepsilon(\mathcal{J}e_h))_{L^2(\Omega)} - s(u_h, e_h).$$

The right-hand side of this is given by (3.15) with $\varphi := \mathcal{J}e_h$. Thus, standard arguments with Cauchy, trace, Poincaré, and Korn inequalities provide

$$(3.21) \quad (\sigma, \varepsilon(\mathcal{J}e_h))_{L^2(\Omega)} - a_h(u_h, e_h) \lesssim (\text{osc}(f, \mathcal{T}) + \text{osc}(g, \mathcal{F}_N)) \|\varepsilon(\mathcal{J}e_h)\|.$$

Since $\mu_0^{1/2} \|\varepsilon(\mathcal{J}e_h)\| \lesssim \|e_h\|_{a_h}$ from Lemma 3.4.b, the combination of (3.19)–(3.21) results in

$$(3.22) \quad \begin{aligned} \|\varepsilon_h e_h\|_{\mathbb{C}} + |e_h|_s + |u_h|_s \\ \lesssim \mu_0^{-1/2} (\|(1 - \Pi_{\mathcal{T}}^k) \sigma\| + |\mathbf{I}u|_s + \mu_0^{-1/2} \text{osc}(f, \mathcal{T}) + \mu_0^{-1/2} \text{osc}(g, \mathcal{F}_N)). \end{aligned}$$

From Lemma 3.6, we infer

$$|\mathbf{I}u|_s \lesssim \|\mu^{1/2} (1 - \Pi_{\mathcal{T}}^k) \varepsilon(u)\| \lesssim \mu_0^{-1/2} \|(1 - \Pi_{\mathcal{T}}^k) \sigma\|.$$

This and (3.22) conclude the proof of (3.17).

3.5.2. Proof of (3.18). Recall from Lemma 3.7.c that $\sigma - \sigma_h \in \Sigma_0$. In view of (3.12), Lemma 3.8, and (3.17), it remains to prove

$$(3.23) \quad \|\mu^{1/2} (\sigma - \sigma_h)\|_{\mathbb{C}^{-1}} \lesssim (\mu_1/\mu_0)^{1/2} (\|(1 - \Pi_{\mathcal{T}}^k) \sigma\| + \text{osc}(f, \mathcal{T}) + \text{osc}(g, \mathcal{F}_N))$$

for (3.18). The Pythagoras theorem with the L^2 orthogonality $\mathbb{C}^{-1/2}(\sigma - \mathbb{C}\varepsilon_h \mathbf{I}u) \perp P_k(\mathcal{T})^{n \times n}$ from Lemma 2.3 proves

$$(3.24) \quad \begin{aligned} \|\mu^{1/2}(\sigma - \sigma_h)\|_{\mathbb{C}^{-1}}^2 &= \|\mu^{1/2}(\sigma - \mathbb{C}\varepsilon_h \mathbf{I}u)\|_{\mathbb{C}^{-1}}^2 + \|\mu^{1/2}\varepsilon_h e_h\|_{\mathbb{C}}^2 \\ &\lesssim \|(1 - \Pi_T^k)\sigma\|^2 + \|\mu^{1/2}\varepsilon_h e_h\|_{\mathbb{C}}^2. \end{aligned}$$

This, the bound $\|\varepsilon_h e_h\|_{\mathbb{C}} \leq \|e_h\|_{a_h}$ from (2.18), and (3.17) imply (3.23). Therefore, we have established (3.18). The combination of (3.17)–(3.18) concludes the proof of Theorem 3.3. \square

3.6. L^2 error estimate. Elliptic regularity allows for L^2 error estimates with higher convergence rates in comparison to Theorem 3.3. We assume that $s > 0$ (index of elliptic regularity) satisfies the following: The solution $z \in H_0^1(\Omega)^n$ to

$$(3.25) \quad -\operatorname{div} \mathbb{C}\varepsilon(z) = f \text{ in } \Omega$$

for any $f \in L^2(\Omega)^n$ satisfies $z \in H^{1+s}(\Omega)^n$ with a regularity index $s > 0$ (depending on the polyhedral domain Ω) and

$$(3.26) \quad \|\mu\varepsilon(z)\|_{H^s(\Omega)} + \|\lambda\operatorname{div} z\|_{H^s(\Omega)} \lesssim c_{\mu,s}\|f\|$$

with a constant $c_{\mu,s}$ depending on μ and s . Such regularity results are available for constant parameters λ and μ under additional assumptions. For instance, (3.26) is established in [12] with $s = 1$ on convex planar domains. Singular functions for general polygonal domains with mixed boundary conditions and $g \equiv 0$ have been computed in [37] and lead to $z \in H^{1+s}(\Omega)^2$ for some explicit $s > 0$ as well as $\|z\|_{H^{1+s}(\Omega)} \lesssim \|f\|$. Thereafter, Lemma 3.7 controls the norm $\lambda\|\operatorname{div} z\|_{H^s(\Omega)}$ and provides (3.26).

While convergence rates of the L^2 error have been derived in [23, Subsection 5.2], the emphasis here is on quasi-best approximation error estimates.

Theorem 3.9 (L^2 error estimate). *If (A) and (3.26), then*

$$(3.27) \quad \|\Pi_{\mathcal{T}}^k u - u_{\mathcal{T}}\| \lesssim c_{\mu,s}\mu_0^{-1}h_{\max}^s (\|(1 - \Pi_{\mathcal{T}}^k)\sigma\| + \operatorname{osc}(f, \mathcal{T}) + \operatorname{osc}(g, \mathcal{F}_N)).$$

Proof. Abbreviate $e_h = (e_{\mathcal{T}}, e_{\mathcal{F}}) := \mathbf{I}u - u_h \in V_h$. Let $z \in V$ solve (3.25) with the right-hand side $e_{\mathcal{T}}$. A consequence of (3.26) and piecewise Poincaré inequalities is

$$(3.28) \quad \|(1 - \Pi_{\mathcal{T}}^k)\mathbb{C}\varepsilon(z)\| \leq 2\|\mu(1 - \Pi_{\mathcal{T}}^k)\varepsilon(z)\| + \|\lambda(1 - \Pi_{\mathcal{T}}^k)\operatorname{div} z\| \lesssim c_{\mu,s}h_{\max}^s \|e_{\mathcal{T}}\|.$$

The L^2 orthogonality $\mathcal{J}e_h - e_{\mathcal{T}} \perp e_{\mathcal{T}}$ and the solution property of z imply

$$(3.29) \quad \begin{aligned} \|e_{\mathcal{T}}\|^2 &= (e_{\mathcal{T}}, \mathcal{J}e_h)_{L^2(\Omega)} = (\mathbb{C}\varepsilon(z), \varepsilon(\mathcal{J}e_h))_{L^2(\Omega)} \\ &= (\mathbb{C}\varepsilon(z), \varepsilon(u) - \varepsilon_h u_h)_{L^2(\Omega)} - (\mathbb{C}\varepsilon(z), \varepsilon(u) - \varepsilon_h \mathbf{I}u + \varepsilon_h e_h - \varepsilon(\mathcal{J}e_h))_{L^2(\Omega)}. \end{aligned}$$

Since $\sigma - \sigma_h = \mathbb{C}(\varepsilon(u) - \varepsilon_h(u_h))$, the first term can be rewritten as $(\mathbb{C}\varepsilon(z), \varepsilon(u) - \varepsilon_h u_h)_{L^2(\Omega)} = (\sigma - \sigma_h, \varepsilon(z))_{L^2(\Omega)}$. This is the left-hand side of (3.15) with $\varphi := z$. Cauchy, Poincaré, and trace inequalities lead to

$$(\mathbb{C}\varepsilon(z), \varepsilon(u) - \varepsilon_h u_h)_{L^2(\Omega)} \lesssim (\operatorname{osc}(f, \mathcal{T}) + \operatorname{osc}(g, \mathcal{F}_N))\|\mathbf{D}_{\text{pw}}(1 - \Pi_{\mathcal{T}}^k)z\| + |u_h|_s |\mathbf{I}z|_s.$$

This, $|\mathbf{I}z|_s \lesssim \|\mu^{1/2}(1 - \Pi_{\mathcal{T}}^k)\varepsilon(z)\|$ from Lemma 3.6, the regularity $z \in H^{1+s}(\Omega)^n$ from (3.26), and $k \geq 1$ provide

$$(3.30) \quad \begin{aligned} &(\mathbb{C}\varepsilon(z), \varepsilon(u) - \varepsilon_h u_h)_{L^2(\Omega)} \\ &\lesssim c_{\mu,s}\mu_0^{-1}h_{\max}^s (\operatorname{osc}(f, \mathcal{T}) + \operatorname{osc}(g, \mathcal{F}_N) + \mu_0^{1/2}|u_h|_s)\|e_{\mathcal{T}}\|. \end{aligned}$$

Recall the L^2 orthogonality $\varepsilon(u) - \varepsilon_h \mathbf{I}u \perp P_k(\mathcal{T})^{n \times n}$ from Lemma 2.3 and $\varepsilon_h e_h - \varepsilon(\mathcal{J}e_h) \perp P_k(\mathcal{T})^{n \times n}$ from Remark 3.5. The Cauchy inequality and (3.28) imply

$$\begin{aligned} & -(\mathbb{C}\varepsilon(z), \varepsilon(u) - \varepsilon_h \mathbf{I}u + \varepsilon_h e_h - \varepsilon(\mathcal{J}e_h))_{L^2(\Omega)} \\ & \leq \|(1 - \Pi_{\mathcal{T}}^k)\mathbb{C}\varepsilon(z)\|(\|(1 - \Pi_{\mathcal{T}}^k)\varepsilon(u)\| + \|\varepsilon_h e_h - \varepsilon(\mathcal{J}e_h)\|) \\ & \lesssim c_{\mu,s} h_{\max}^s (\|(1 - \Pi_{\mathcal{T}}^k)\varepsilon(u)\| + \|\varepsilon_h e_h - \varepsilon(\mathcal{J}e_h)\|) \|e_{\mathcal{T}}\|. \end{aligned}$$

This, the stability $\|\varepsilon_h e_h - \varepsilon(\mathcal{J}e_h)\| \lesssim \mu_0^{-1/2} \|e_h\|_{a_h}$ from Lemma 3.4, and $2\mu_0 \|(1 - \Pi_{\mathcal{T}}^k)\varepsilon(u)\| \leq \|(1 - \Pi_{\mathcal{T}}^k)\sigma\|$ establish

$$(3.31) \quad \begin{aligned} & -(\mathbb{C}\varepsilon(z), \varepsilon(u) - \varepsilon_h \mathbf{I}u + \varepsilon_h e_h - \varepsilon(\mathcal{J}e_h))_{L^2(\Omega)} \\ & \lesssim c_{\mu,s} \mu_0^{-1} h_{\max}^s (\|(1 - \Pi_{\mathcal{T}}^k)\sigma\| + \mu_0^{1/2} \|e_h\|_{a_h}) \|e_{\mathcal{T}}\|. \end{aligned}$$

The combination of (3.29)–(3.31) with (1.3) concludes the proof. \square

3.7. Quasi-best approximation with smoother. If the given data $f \in V^*$ or $g \in \tilde{H}^{-1/2}(\Gamma_N)^n$ is non-smooth, then the operator \mathcal{J} can be utilized in an alternative HHO method in the spirit of [40, 29]. The continuous problem seeks $u \in V$ such that any $v \in V$ satisfies

$$(3.32) \quad (\mathbb{C}\varepsilon(u), \varepsilon(v))_{L^2(\Omega)} = \langle f, v \rangle_{V^* \times V} + \langle g, v \rangle_{\tilde{H}^{-1/2}(\Gamma_N) \times \tilde{H}^{1/2}(\Gamma_N)}.$$

The corresponding discrete problem seeks $u_h \in V_h$ with

$$(3.33) \quad a_h(u_h, v_h) = \langle f, \mathcal{J}v_h \rangle_{V^* \times V} + \langle g, \mathcal{J}v_h \rangle_{\tilde{H}^{-1/2}(\Gamma_N) \times \tilde{H}^{1/2}(\Gamma_N)}$$

for any $v_h \in V_h$. Let $\sigma = \mathbb{C}\varepsilon(u)$ and $\sigma_h = \mathbb{C}\varepsilon_h u_h$ denote the continuous and discrete stress variable. The arguments of this section imply the following oscillation-free and λ -robust quasi-best approximation error estimate.

Theorem 3.10 (a priori with smoother). *If (A) and (3.26) hold, then*

$$(3.34) \quad \begin{aligned} & (\mu_0/\mu_1)^{1/2} \|\sigma - \sigma_h\| + \mu_0^{1/2} \|\mathbf{I}u - u_h\|_{a_h} + \mu_0^{1/2} |u_h|_s + c_{\mu,s}^{-1} \mu_0 h_{\max}^{-s} \|\Pi_{\mathcal{T}}^k u - u_{\mathcal{T}}\| \\ & \lesssim \|(1 - \Pi_{\mathcal{T}}^k)\sigma\|. \end{aligned}$$

Proof. The arguments in the proof of Theorem 3.3 apply to this case as well with the following adjustments. Abbreviate $e_h := \mathbf{I}u - u_h \in V_h$. First, observe from the variational formulations (3.32)–(3.33) that

$$(\sigma, \varepsilon(\mathcal{J}e_h))_{L^2(\Omega)} - a_h(u_h, e_h) = 0.$$

Therefore, the data oscillations in (3.21) do not arise and

$$(3.35) \quad \|e_h\|_{a_h} + |u_h|_s \lesssim \mu_0^{-1/2} \|(1 - \Pi_{\mathcal{T}}^k)\sigma\|$$

holds instead of (3.22). The second observation is the projection property

$$\Pi_{\mathcal{T}}^k \varepsilon(\mathcal{J}\mathbf{I}\varphi) = \varepsilon_h \mathbf{I}\varphi = \Pi_{\mathcal{T}}^k \varepsilon(\varphi)$$

for all $\varphi \in V$ from Lemma 2.3 and $\mathbf{I} \circ \mathcal{J} = \text{Id}$ by design of the right-inverse \mathcal{J} . This, $\sigma_h \in P_k(\mathcal{T})^{n \times n}$, and the variational formulations (3.32)–(3.33) reveal

$$(3.36) \quad (\sigma - \sigma_h, \varepsilon(\mathcal{J}\mathbf{I}\varphi))_{L^2(\Omega)} = (\sigma, \varepsilon(\mathcal{J}\mathbf{I}\varphi))_{L^2(\Omega)} - (\sigma_h, \varepsilon_h \mathbf{I}\varphi)_{L^2(\Omega)} = -s(u_h, \mathbf{I}\varphi).$$

Recall $|\mathbf{I}\varphi|_s \lesssim \mu_1^{1/2} \|\varepsilon(\varphi)\|$ from Theorem 2.1 and $\mu_0^{1/2} |u_h|_s \lesssim \|(1 - \Pi_{\mathcal{T}}^k)\sigma\|$ from (3.35). Therefore, a Cauchy inequality in (3.36) provides

$$(\sigma - \sigma_h, \varepsilon(\mathcal{J}\mathbf{I}\varphi))_{L^2(\Omega)} \lesssim (\mu_1/\mu_0)^{1/2} \|(1 - \Pi_{\mathcal{T}}^k)\sigma\| \|\varepsilon(\varphi)\|.$$

The combination of this with $\varepsilon(\varphi - \mathcal{I}\varphi) \perp P_k(\mathcal{T})^{n \times n}$, $\|\varepsilon(\varphi - \mathcal{I}\varphi)\| \lesssim \|\varepsilon(\varphi)\|$ from (3.8), and a Cauchy inequality result in

$$\begin{aligned} (\sigma - \sigma_h, \varepsilon(\varphi))_{L^2(\Omega)} &= ((1 - \Pi_{\mathcal{T}}^k)\sigma, \varepsilon(\varphi - \mathcal{I}\varphi))_{L^2(\Omega)} - (\sigma - \sigma_h, \varepsilon(\mathcal{I}\varphi)) \\ &\lesssim (\mu_1/\mu_0)^{1/2} \|(1 - \Pi_{\mathcal{T}}^k)\sigma\| \|\varepsilon(\varphi)\|. \end{aligned}$$

The supremum of this over all $\varphi \in H_0^1(\Omega)^n$ with the normalization $\|\mathbf{D}\varphi\| = 1$ provides $\|\operatorname{div}(\sigma - \sigma_h)\|_{-1} \lesssim (\mu_1/\mu_0)^{1/2} \|(1 - \Pi_{\mathcal{T}}^k)\sigma\|$. This, (3.24), and $\|\varepsilon_h e_h\|_{\mathbb{C}} \leq \|e_h\|_{a_h} \lesssim \mu_0^{-1/2} \|(1 - \Pi_{\mathcal{T}}^k)\sigma\|$ from (3.35) imply

$$\|\mu^{1/2}(\sigma - \sigma_h)\|_{\mathbb{C}^{-1}}^2 \lesssim (\mu_1/\mu_0) \|(1 - \Pi_{\mathcal{T}}^k)\sigma\|^2.$$

For the modified HHO method (3.33), (3.14) holds verbatim and this leads to $\sigma - \sigma_h \in \Sigma_0$ as in Lemma 3.7.c. In view of (3.12), we have proven $\|\sigma - \sigma_h\| \lesssim (\mu_1/\mu_0)^{1/2} \|(1 - \Pi_{\mathcal{T}}^k)\sigma\|$. This and (3.35) conclude the proof of

$$(3.37) \quad (\mu_0/\mu_1)^{1/2} \|\sigma - \sigma_h\| + \mu_0^{1/2} \|e_h\|_{a_h} + \mu_0^{1/2} |u_h|_s \lesssim \|(1 - \Pi_{\mathcal{T}}^k)\sigma\|.$$

To derive L^2 estimates, adopt the notation of z and e_h from the proof of Theorem 3.9. Recall that $(\mathbb{C}\varepsilon(z), \varepsilon(u) - \varepsilon_h u_h)_{L^2(\Omega)} = (\sigma - \sigma_h, \varepsilon(z))_{L^2(\Omega)} \leq |u_h|_s |\mathbf{I}z|_s$ from (3.36). The regularity (3.26) and Lemma 3.6.a allow for $|\mathbf{I}z|_s \lesssim \|\mu^{1/2}(1 - \Pi_{\mathcal{T}}^k)\varepsilon(z)\| \lesssim c_{\mu,s} \mu_0^{-1/2} h_{\max}^s \|e_{\mathcal{T}}\|$. Therefore,

$$(3.38) \quad (\mathbb{C}\varepsilon(z), \varepsilon(u) - \varepsilon_h u_h)_{L^2(\Omega)} \lesssim c_{\mu,s} \mu_0^{-1/2} h_{\max}^s |u_h|_s \|e_{\mathcal{T}}\|.$$

Since (3.29) and (3.31) only involve the orthogonality arising from Lemma 2.3 and Lemma 3.4, they hold verbatim. The combination of this with (3.37)–(3.38) reveals $\|\Pi_{\mathcal{T}}^k u - u_{\mathcal{T}}\| \lesssim c_{\mu,s} \mu_0^{-1} h_{\max}^s \|(1 - \Pi_{\mathcal{T}}^k)\sigma\|$. \square

4. STABILIZATION-FREE AND λ -ROBUST A POSTERIORI ERROR ANALYSIS

This section derives the λ -robust reliable and efficient error estimate η from (1.5).

4.1. Main result. The main result of this section establishes the a posteriori error estimate (1.4) for the discretization (2.17) without smoother.

Theorem 4.1 (a posteriori). *Suppose (A), then (1.4) holds with λ -independent constants C_{rel} and C_{eff} that exclusively depend on k , Γ_{D} , Σ_0 , and \mathbb{T} .*

Remark 4.2 (a posteriori with smoother). For the discretization (3.33) with smoother and L^2 right-hand sides, Theorem 4.1 holds verbatim. The situation is, unfortunately, much more involved for H^{-1} right-hand sides, where explicit error control relies on additional a priori information on f . We omit further comments on such cases, but refer to [32] for an abstract approach and [19] for explicit examples.

Remark 4.3 (Comparison with [4]). The only other stabilisation-free a posteriori error analysis for some HHO method applied to second-order PDE is [4] on the Poisson model problem with an orthogonality of the piecewise gradients of some representation $\mathcal{R}u_h$ of the HHO displacement u_h to divergence-free lowest-order Raviart-Thomas finite element functions. It is however difficult to mimic the Helmholtz decomposition from [4], which is in particular challenging in 3D and in presence of mixed boundary conditions.

Remark 4.4 (other applications). The a posteriori error analysis of this section can be extended to the scalar elliptic PDE $-\operatorname{div} A \nabla u = f$ in Ω , $u = 0$ on Γ_{D} , $\sigma \nu = g$ on Γ_{N} with the stress $\sigma = A \nabla u$ and pointwise symmetric positive definite coefficients $A \in P_0(\mathcal{T})^{n \times n}$. Let the discrete solution $u_h \in V_h$ solve

$$\int_{\Omega} A \mathcal{G} u_h \cdot \mathcal{G} v_h = \int_{\Omega} f v_{\mathcal{T}} \, dx + \int_{\Gamma_{\text{N}}} g v_{\mathcal{F}} \, ds \quad \text{for any } v_h = (v_{\mathcal{T}}, v_{\mathcal{F}}) \in V_h,$$

where the notation of this paper is carried over to the scalar case. Then our analysis below establishes that the discrete stress $\sigma_h := A\mathcal{G}_h u_h$ satisfies

$$\begin{aligned} \|\sigma - \sigma_h\|_{A^{-1}}^2 &\lesssim \|h_{\mathcal{T}}(f + \operatorname{div}_{\text{pw}}\sigma_h)\|^2 + \min_{v \in V} \|\nabla v - \mathcal{G}_h u_h\|_A^2 \\ &\quad + \sum_{F \in \mathcal{F}(\Omega)} h_F \|[\sigma_h]_{F\nu_F}\|_{L^2(F)}^2 + \sum_{F \in \mathcal{F}_N} h_F \|g - \sigma_h \nu_F\|_{L^2(F)}^2 \\ &\lesssim \|\sigma - \sigma_h\|_{A^{-1}}^2 + \operatorname{osc}^2(f, \mathcal{T}) + \operatorname{osc}^2(g, \mathcal{F}_N) \end{aligned}$$

with the weighted norm $\|\bullet\|_{A^s} := (A^s \bullet, \bullet)_{L^2(\Omega)}$ for $s = \pm 1$.

4.2. Proof of reliability. The proof is divided into three steps.

4.2.1. Orthogonal split. Recall $\psi \in V$ from Lemma 3.7.d and define the divergence free function $\tau := \sigma - \sigma_h - \mathbb{C}\varepsilon(\psi) \in L^2(\Omega)^{n \times n}$ with the L^2 orthogonality $\tau \perp \varepsilon(V)$. The latter is equivalent to the L^2 orthogonality $\mathbb{C}^{-1/2}\tau \perp \mathbb{C}^{1/2}\varepsilon(V)$ and the Pythagoras theorem provides the split

$$(4.1) \quad \|\sigma - \sigma_h\|_{\mathbb{C}^{-1}}^2 = \|\varepsilon(\psi)\|_{\mathbb{C}}^2 + \|\tau\|_{\mathbb{C}^{-1}}^2.$$

4.2.2. Proof of

$$(4.2) \quad \mu_0^{1/2} \|\varepsilon(\psi)\|_{\mathbb{C}} + \|\operatorname{div}(\sigma - \sigma_h)\|_{-1} \lesssim \eta.$$

Given any $\varphi \in V$, let $\varphi_{\mathbb{C}} \in S_{\mathbb{D}}^1(\mathcal{T})$ denote the Scott-Zhang quasi-interpolation [38] of φ with the local approximation property

$$(4.3) \quad h_T \|\varphi - \varphi_{\mathbb{C}}\|_{L^2(T)} + \|\mathbb{D}(\varphi - \varphi_{\mathbb{C}})\|_{L^2(T)} \lesssim \|\mathbb{D}\varphi\|_{L^2(\Omega(T))}$$

in the element patch $\Omega(T)$. Since $\varphi_{\mathbb{C}} \in S_{\mathbb{D}}^1(\mathcal{T})$, $(\sigma - \sigma_h, \varepsilon(\varphi_{\mathbb{C}}))_{L^2(\Omega)} = 0$ from (3.15) and Corollary 2.2. An integration by parts reveals

$$\begin{aligned} (\sigma - \sigma_h, \varepsilon(\varphi))_{L^2(\Omega)} &= (\sigma - \sigma_h, \varepsilon(\varphi - \varphi_{\mathbb{C}}))_{L^2(\Omega)} = (\sigma - \sigma_h, \mathbb{D}(\varphi - \varphi_{\mathbb{C}}))_{L^2(\Omega)} \\ &= (f + \operatorname{div}_{\text{pw}}\sigma_h, \varphi - \varphi_{\mathbb{C}})_{L^2(\Omega)} \\ &\quad + \sum_{F \in \mathcal{F}(\Omega)} (\varphi - \varphi_{\mathbb{C}}, [\sigma_h]_{F\nu_F})_{L^2(F)} + \sum_{F \in \mathcal{F}_N} (\varphi - \varphi_{\mathbb{C}}, g - \sigma_h \nu_F)_{L^2(F)}. \end{aligned}$$

Standard arguments in the a posteriori error analysis with the Cauchy and trace inequalities as well as with (4.3) result in

$$(4.4) \quad \begin{aligned} (\sigma - \sigma_h, \varepsilon(\varphi))_{L^2(\Omega)} &\lesssim \|h_{\mathcal{T}}(f + \operatorname{div}_{\text{pw}}\sigma_h)\| \|\mathbb{D}\varphi\| \\ &\quad + \left(\sum_{F \in \mathcal{F}(\Omega)} h_F \|[\sigma_h]_{F\nu_F}\|_{L^2(F)}^2 + \sum_{F \in \mathcal{F}_N} h_F \|g - \sigma_h \nu_F\|_{L^2(F)}^2 \right)^{1/2} \|\mathbb{D}\varphi\|. \end{aligned}$$

This proves $\|\operatorname{div}(\sigma - \sigma_h)\|_{-1} \lesssim \eta$. The definition of ψ in Lemma 3.7.a implies $\|\varepsilon(\psi)\|_{\mathbb{C}}^2 = (\sigma - \sigma_h, \varepsilon(\psi))_{L^2(\Omega)}$. Since $\|\mathbb{D}\psi\| \lesssim \|\varepsilon(\psi)\| \lesssim \mu_0^{-1/2} \|\varepsilon(\psi)\|_{\mathbb{C}}$ from the (first) Korn inequality (1.7), $\|\varepsilon(\psi)\|_{\mathbb{C}} \lesssim \mu_0^{-1/2} \eta$ follows from (4.4) with the choice $\varphi := \psi$.

4.2.3. Proof of

$$(4.5) \quad \mu_0^{1/2} \|\tau\|_{\mathbb{C}^{-1}} \lesssim (\mu_1/\mu_0)^{1/2} \eta.$$

The L^2 orthogonality $\mathbb{C}^{-1}\tau \perp \mathbb{C}\varepsilon(V)$ from the definition of ψ in Lemma 3.7.d and a Cauchy inequality provide, for any $v \in V$, that

$$(4.6) \quad \begin{aligned} \|\tau\|_{\mathbb{C}^{-1}}^2 &= (\mathbb{C}\varepsilon(v) - \sigma_h, \mathbb{C}^{-1}\tau)_{L^2(\Omega)} = (\varepsilon(v) - \varepsilon_h u_h, \tau)_{L^2(\Omega)} \\ &\leq \mu_0^{-1/2} \|\mu^{1/2}(\varepsilon(v) - \varepsilon_h u_h)\| \|\tau\|. \end{aligned}$$

Since $\sigma - \sigma_h$ and $\mathbb{C}\varepsilon(\psi)$ are contained in Σ_0 from Lemma 3.7.c-d, $\tau = \sigma - \sigma_h - \mathbb{C}\varepsilon(\psi) \in \Sigma_0$. Hence, Lemma 3.7.b implies $\|\tau\| \lesssim \|\mu^{1/2}\tau\|_{\mathbb{C}^{-1}} + \|\operatorname{div}\tau\|_{-1}$. This,

(4.6), and $\operatorname{div} \tau = 0$ conclude the proof of (4.5).

Finish of the proof The bound $\|\sigma - \sigma_h\| \lesssim \|\mu^{1/2}(\sigma - \sigma_h)\|_{\mathbb{C}^{-1}} + \|\operatorname{div}(\sigma - \sigma_h)\|_{-1}$ from (3.12), (4.1)–(4.2), and (4.5) conclude the proof of $\|\sigma - \sigma_h\| \lesssim (\mu_1/\mu_0)\eta$. \square

4.3. Proof of efficiency. We establish the efficiency of η from (1.5) with the choice $v := \mathcal{A}u_h$. The proof is divided into three parts: the first one is devoted to the efficiency of nodal averaging (without stabilization) while the remaining parts establish the efficiency of the remaining terms with bubble function techniques [44].

4.3.1. Efficiency of nodal averaging. A straightforward modification of the proof of [26, Theorem 4.7] using (3.5) and Theorem 2.1 leads to

$$(4.7) \quad \begin{aligned} \|\mathbf{D}_{\text{pw}}(\mathcal{R} - \mathcal{A})u_h\| &\lesssim \min_{v \in V} \|\mathbf{D}_{\text{pw}}(v - \mathcal{R}u_h)\| + \tilde{s}(u_h, u_h)^{1/2} \\ &\lesssim \|\mathbf{D}_{\text{pw}}(\mathcal{J}u_h - \mathcal{R}u_h)\| + |u_h|_{\tilde{s}} \end{aligned}$$

with the right-inverse \mathcal{J} of \mathbf{I} from Lemma 3.4 and the stabilization \tilde{s} from (2.8). Since $\mathbf{I}\mathcal{J}u_h = u_h$, (2.16) provides

$$\|\mathbf{D}_{\text{pw}}(\mathcal{J}u_h - \mathcal{R}u_h)\| \lesssim \|\varepsilon_{\text{pw}}(\mathcal{J}u_h - \mathcal{R}u_h)\|.$$

Recall the best approximation property in (2.16) to obtain

$$\|\varepsilon_{\text{pw}}(\mathcal{J}u_h - \mathcal{R}u_h)\| \leq \|\varepsilon_{\text{pw}}(\mathcal{J}u_h - \mathcal{R}\mathbf{I}u)\| \leq \|\varepsilon(\mathcal{J}u_h - \mathcal{J}\mathbf{I}u)\| + \|\varepsilon_{\text{pw}}(\mathcal{J} - \mathcal{R})\mathbf{I}u\|.$$

The combination of the two previously displayed formula with the stability $\|\varepsilon(\mathcal{J}u_h - \mathcal{J}\mathbf{I}u)\| \lesssim \|\mathbf{I}u - u_h\|_h$ and $\|\varepsilon_{\text{pw}}(\mathcal{J}\mathbf{I}u - \mathcal{R}\mathbf{I}u)\| \lesssim \|\mathbf{D}_{\text{pw}}(u - \mathcal{R}\mathbf{I}u)\| + |\mathbf{I}u|_{\tilde{s}}$ from Lemma 3.4 results in

$$\|\mathbf{D}_{\text{pw}}(\mathcal{J}u_h - \mathcal{R}u_h)\| \lesssim \|\mathbf{I}u - u_h\|_h + \|\mathbf{D}_{\text{pw}}(u - \mathcal{R}\mathbf{I}u)\| + |\mathbf{I}u|_{\tilde{s}}.$$

This, (4.7), $\|\mathbf{D}_{\text{pw}}(u - \mathcal{R}\mathbf{I}u)\| \lesssim \|\varepsilon_{\text{pw}}(u - \mathcal{R}\mathbf{I}u)\|$ from (2.16), $\|\mathbf{I}u - u_h\|_h \lesssim \mu_0^{-1/2}\|\mathbf{I}u - u_h\|_{a_h}$ from Theorem 2.7, and $\|\varepsilon_{\text{pw}}(\mathcal{R}u_h - \mathcal{A}u_h)\| \leq \|\mathbf{D}_{\text{pw}}(\mathcal{R}u_h - \mathcal{A}u_h)\|$ imply

$$(4.8) \quad \|\varepsilon_{\text{pw}}(\mathcal{R}u_h - \mathcal{A}u_h)\| \lesssim \|\varepsilon_{\text{pw}}(u - \mathcal{R}\mathbf{I}u)\| + \mu_0^{-1/2}\|\mathbf{I}u - u_h\|_{a_h} + |u_h|_{\tilde{s}} + |\mathbf{I}u|_{\tilde{s}}.$$

From Lemma 2.6 and a triangle inequality, we deduce that $\|\varepsilon_h u_h - \varepsilon(\mathcal{A}u_h)\| \lesssim \|\varepsilon_{\text{pw}}(\mathcal{R}u_h - \mathcal{A}u_h)\| + |u_h|_{\tilde{s}}$. Hence, the a priori result $\mu_0^{1/2}|u_h|_{\tilde{s}} \leq \mu_0^{1/2}\|\mathbf{I}u - u_h\|_{a_h} \lesssim \|\sigma - \sigma_h\| + \operatorname{osc}(f, \mathcal{T}) + \operatorname{osc}(g, \mathcal{F}_N)$ from (1.3), the quasi-optimality $|\mathbf{I}u|_{\tilde{s}} + \|\varepsilon_{\text{pw}}(u - \mathcal{R}\mathbf{I}u)\| \lesssim \|(1 - \Pi_{\mathcal{T}}^k)\varepsilon(u)\|$ from (3.7), and (4.8) show

$$(4.9) \quad (\mu_0/\mu_1)\|\mu(\varepsilon_h u_h - \varepsilon(\mathcal{A}u_h))\| \lesssim \|\sigma - \sigma_h\| + \operatorname{osc}(f, \mathcal{T}) + \operatorname{osc}(g, \mathcal{F}_N).$$

4.3.2. Efficiency of Neumann data approximation. Given $F \in \mathcal{F}_N$, let $T \in \mathcal{T}$ be the unique simplex with $F \in \mathcal{F}(T)$. Abbreviate $e_k := \Pi_F^k g - \sigma_h \nu_F \in P_k(F)^n$. There exists $\varphi \in H^1(\Omega)^n$ with $\varphi = 0$ in $\Omega \setminus T$, $\Pi_F^k \varphi = h_F e_k$, and

$$(4.10) \quad \|\mathbf{D}\varphi\|_{L^2(T)} \lesssim h_F^{-1}\|\varphi\|_{L^2(T)} \lesssim h_F^{-1/2}\|\varphi\|_{L^2(F)} \lesssim h_F^{1/2}\|e_k\|_{L^2(F)}$$

as in [29, Subsection 4.3]. An integration by parts and a Cauchy inequality show

$$\begin{aligned} ((\sigma - \sigma_h)\nu_F, \varphi)_{L^2(F)} &= (f + \operatorname{div} \sigma_h, \varphi)_{L^2(T)} + (\sigma - \sigma_h, \mathbf{D}\varphi)_{L^2(T)} \\ &\leq \|f + \operatorname{div} \sigma_h\|_{L^2(T)}\|\varphi\|_{L^2(T)} + \|\sigma - \sigma_h\|_{L^2(T)}\|\mathbf{D}\varphi\|_{L^2(T)}. \end{aligned}$$

Since $h_F\|e_k\|_{L^2(F)}^2 = ((\sigma - \sigma_h)\nu_F, \varphi)_{L^2(F)} + ((1 - \Pi_F^k)g, \varphi)_{L^2(F)}$ from $\sigma \nu_F = g$ on F , this, a Cauchy inequality, and (4.10) reveal

$$h_F^{1/2}\|e_k\|_{L^2(F)} \lesssim h_T\|f + \operatorname{div} \sigma_h\|_{L^2(T)} + \|\sigma - \sigma_h\|_{L^2(T)} + h_F^{1/2}\|(1 - \Pi_F^k)g\|_{L^2(F)}.$$

Therefore, the Pythagoras theorem provides

$$(4.11) \quad \begin{aligned} h_F\|g - \sigma_h \nu_F\|_{L^2(F)}^2 &= h_F\|(1 - \Pi_F^k)g\|_{L^2(F)}^2 + h_F\|e_k\|_{L^2(F)}^2 \\ &\lesssim h_F\|(1 - \Pi_F^k)g\|_{L^2(F)}^2 + \|h_{\mathcal{T}}(f + \operatorname{div} \sigma_h)\|_{L^2(T)}^2 + \|\sigma - \sigma_h\|_{L^2(T)}^2. \end{aligned}$$

4.3.3. *Finish of the proof.* The efficiency $h_T \|f + \operatorname{div} \sigma_h\|_{L^2(F)} \lesssim \|\sigma - \sigma_h\| + h_T \|(1 - \Pi_T^k) f\|_{L^2(T)}$ for any $T \in \mathcal{T}$ has been established in [4, Proof of Theorem 2] for the Poisson equation. An extension to the case at hand is straightforward. The efficiency $h_F^{1/2} \|[\sigma_h] \nu_F\|_{L^2(F)}^2 \lesssim \|\sigma - \sigma_h\|_{L^2(\omega(F))} + \|h_{\mathcal{T}}(f + \operatorname{div}_{\text{pw}} \sigma_h)\|_{L^2(\omega(F))}$ can be established with the arguments from [44, Section 1.4.5]. Further details on these two terms are therefore omitted. In combination with (4.9) and (4.11), we conclude $(\mu_0/\mu_1)\eta \lesssim \|(1 - \Pi_{\mathcal{T}}^k)\sigma\| + \operatorname{osc}(f, \mathcal{T}) + \operatorname{osc}(g, \mathcal{F}_N)$. \square

4.4. **Extension to inhomogeneous Dirichlet boundary data in 2D.** In the following, we derive reliable error estimates for inhomogeneous Dirichlet boundary data in 2D. We assume that Γ_D lies on one connectivity component of $\partial\Omega$. Given $u_D \in C(\Gamma_D)^2 \cap H^1(\mathcal{F}_D)^2$, $f \in L^2(\Omega)^2$, and $g \in L^2(\Gamma_N)^2$, the continuous (resp. discrete) problem seeks the exact (resp. discrete) solution $u \in u_D + V$ (resp. $u_h \in I_D u_D + V_h$) to (1.2) (resp. (2.17)). (Here, u_D is understood as an H^1 extension in the domain Ω .) The proof of reliability in Subsection 4.2 and the observation $\mathbb{C}^{-1}\tau \perp \mathbb{C}\varepsilon(u_D + V)$ (instead of $\mathbb{C}^{-1}\tau \perp \mathbb{C}\varepsilon(V)$ in (4.6)) lead to

$$(4.12) \quad \|\sigma - \sigma_h\| \lesssim (\mu_1/\mu_0)\eta$$

with η from (1.5), where the minimum in (1.5) is taken over the set $u_D + V$ (instead of V). Let $I_D u_D$ denote the nodal interpolation of u_D in $P_{k+1}(\mathcal{F}_D)^2 \cap C(\Gamma_D)^2$. We choose the nodal average $v := \mathcal{A}u_h$ of $\mathcal{R}u_h$ in (4.12); the degrees of freedom of $\mathcal{A}u_h$ on Γ_D are fixed by the point evaluation of u_D so that $\mathcal{A}u_h|_{\Gamma_D} = I_D u_D$. Since $I_D u_D \neq u_D$ in general, additional error quantities occur. A triangle inequality shows

$$(4.13) \quad \min_{w \in u_D + V} \|\varepsilon(w) - \varepsilon_h u_h\| \leq \min_{w \in u_D + V} \|\varepsilon(w) - \varepsilon(\mathcal{A}u_h)\| + \|\varepsilon(\mathcal{A}u_h) - \varepsilon_h u_h\|.$$

The minimizer z of $\|\varepsilon(w) - \varepsilon(\mathcal{A}u_h)\|$ among $w \in u_D + V$ defines $\varrho := \varepsilon(z) - \varepsilon(\mathcal{A}u_h) \in L^2(\Omega)^2$ with the boundary condition $(z - \mathcal{A}u_h)|_{\Gamma_D} = u_D - I_D u_D$ and L^2 orthogonality $\varrho \perp DV$ from the Euler-Lagrange equations. Therefore, $\operatorname{div} \varrho = 0$ in Ω and $\varrho \nu = 0$ along Γ_N . The Helmholtz decomposition [17, Lemma 3.1] shows the existence of $\beta = (\beta_1, \beta_2) \in H^1(\Omega)^2$ (even as a Curl of an H^2 function) with

$$(4.14) \quad \operatorname{Curl} \beta = \begin{pmatrix} \partial_2 \beta_1 & -\partial_1 \beta_1 \\ \partial_2 \beta_2 & -\partial_1 \beta_2 \end{pmatrix} = \varrho, \quad \|\beta\|_{H^1(\Omega)} \lesssim \|\varrho\|, \quad \text{and}$$

β is constant on each connectivity component of Γ_N , i.e., $\partial\beta/\partial s = 0$ on $\operatorname{relint}(\Gamma_N)$. (The assumptions in [17] that (a) Γ_D is connected and (b) Γ_N and Γ_D have positive distance, can be relaxed to the present one with the arguments from here and [17].) The a.e. pointwise symmetry of $\operatorname{Curl} \beta$ and an integration by parts reveal

$$\begin{aligned} \|\varrho\|^2 &= (\varrho, \operatorname{Curl} \beta)_{L^2(\Omega)} = (Dz - D\mathcal{A}u_h, \operatorname{Curl} \beta)_{L^2(\Omega)} \\ &= - \int_{\partial\Omega} (z - \mathcal{A}u_h) \cdot \partial\beta/\partial s \, ds = - \int_{\Gamma_D} (u_D - I_D u_D) \cdot \partial\beta/\partial s \, ds \\ &= - \sum_{F \in \mathcal{F}_D} \int_F (u_D - I_D u_D) \cdot \partial\beta/\partial s \, ds, \end{aligned}$$

because $(u_D - I_D u_D)|_F \in H_0^1(F)^2$ on $F \in \mathcal{F}_D$ and $\partial\beta/\partial s \in H^{-1/2}(\partial\Omega)$ vanishes on Γ_N (written $\partial\beta/\partial s \in \tilde{H}^{-1/2}(\Gamma_D)^2$ as its zero extension belongs to $H^{-1/2}(\partial\Omega)$). This holds at least for smooth β , where an edge-wise integration by parts shows

$$(4.15) \quad \|\varrho\|^2 = (D(z - \mathcal{A}u_h), \operatorname{Curl} \beta)_{L^2(\Omega)} = \sum_{F \in \mathcal{F}_D} \int_F \beta \cdot \partial(u_D - I_D u_D)/\partial s \, ds.$$

The second equation (4.15.b) in (4.15) holds for all smooth functions β with $\partial\beta/\partial s = 0$ on Γ_N . Since those functions can approximate $\beta \in H^1(\Omega)^2$ from (4.14) (by density in $H^1(\Omega)^2$ even with the side restriction that β is constant on each connectivity

component of Γ_N), (4.15.b) holds for β from (4.14) as well. Nodal interpolation leads to $\int_F \partial(u_D - I_D u_D)/\partial s ds = 0$ for any $F \in \mathcal{F}_D$ with the fundamental theorem of calculus along the 1D edge F . This and the Cauchy inequality in (4.15) provide

$$(4.16) \quad \begin{aligned} \|\varrho\|^2 &\leq \sum_{F \in \mathcal{F}_D} \|(1 - \Pi_F^0)\beta\|_{L^2(F)} \|\partial(u_D - I_D u_D)/\partial \tau\|_{L^2(F)} \\ &\leq \left(\sum_{F \in \mathcal{F}_D} h_F^{-1} \|(1 - \Pi_F^0)\beta\|_{L^2(F)}^2 \right)^{1/2} \text{osc}(u_D, \mathcal{F}_D) \end{aligned}$$

with $\text{osc}(u_D, \mathcal{F}_D)^2 := \sum_{F \in \mathcal{F}_D} h_F \|\partial(u_D - I_D u_D)/\partial s\|_{L^2(F)}^2$. Given $F \in \mathcal{F}_D$, let $T_F \in \mathcal{T}$ be the unique triangle with $F \in \mathcal{F}(T_F)$. A trace and Poincaré inequality imply

$$\sum_{F \in \mathcal{F}_D} h_F^{-1} \|(1 - \Pi_F^0)\beta\|_{L^2(F)}^2 \leq \sum_{F \in \mathcal{F}_D} h_F^{-1} \|(1 - \Pi_{T_F}^0)\beta\|_{L^2(F)}^2 \lesssim \|D\beta\|^2 \lesssim \|\varrho\|^2$$

with (4.14) in the last step. From this and (4.16), we infer

$$\|\varrho\| \lesssim \text{osc}(u_D, \mathcal{F}_D).$$

This and (4.12)–(4.13) reveal the reliability of the error estimator $\tilde{\eta}$,

$$(4.17) \quad \begin{aligned} (\mu_0/\mu_1)^2 \|\sigma - \sigma_h\|^2 &\lesssim \tilde{\eta}^2 := \|h_{\mathcal{T}}(f + \text{div}_{\text{pw}} \sigma_h)\|^2 + \|\mu(\varepsilon(\mathcal{A}u_h) - \varepsilon_h u_h)\|^2 \\ &+ \sum_{F \in \mathcal{F}(\Omega)} h_F \|[\sigma_h]_F \nu_F\|_{L^2(F)}^2 + \sum_{F \in \mathcal{F}_N} h_F \|g - \sigma_h \nu_F\|_{L^2(F)}^2 + \mu_1^2 \text{osc}(u_D, \mathcal{F}_D)^2. \end{aligned}$$

5. NUMERICAL EXAMPLES

This section provides two numerical benchmarks in 2D with locking behaviour observed in [13] for low-order conforming FEM.

5.1. Preliminary remarks. The material parameters λ, μ are given by the formulas $\lambda = E\nu/((1 + \nu)(1 - 2\nu))$ and $\mu = E/(2(1 + \nu)) \rightarrow \infty$ as $\nu \rightarrow 1/2$ with the default Young's modulus $E = 10^5$ and the Poisson ratio $\nu = 0.4999$. The only exceptions of those parameters are in Figure 2.b and Figure 5.b, where $\nu = 0.4999$ is displayed as well as numerical results for $\nu = 0.3$ for comparison.

Adaptive computations utilize the refinement indicator

$$(5.1) \quad \begin{aligned} \eta^2(T) &:= \|h_T(f + \text{div} \sigma_h)\|_{L^2(T)}^2 + (\mu|_T)^2 \|\varepsilon(\mathcal{A}u_h) - \varepsilon_h u_h\|_{L^2(T)}^2 \\ &+ \sum_{F \in \mathcal{F}(T) \cap \mathcal{F}(\Omega)} h_F \|[\sigma_h]_F \nu_F\|_{L^2(F)}^2 + \sum_{F \in \mathcal{F}(T) \cap \mathcal{F}_N} h_F \|g - \sigma_h \nu_F\|_{L^2(F)}^2 \end{aligned}$$

for $T \in \mathcal{T}$ with $\mathcal{T} \in \mathbb{T}$ arising from the error estimator (1.5) with the average $\mathcal{A}u_h$ of $\mathcal{R}u_h$. A standard adaptive loop [27] with the Dörfler marking strategy determines a subset \mathcal{M} of minimal cardinality such that

$$\sum_{T \in \mathcal{T}} \eta^2(T) \leq \frac{1}{2} \sum_{T \in \mathcal{M}} \eta^2(T).$$

The convergence history plots display the quantities of interest against the number of degrees of freedom (**ndof**) in a log-log plot. (Recall the scaling $\text{ndof} \approx h_{\max}^{-2}$ for uniform meshes in 2D.) Solid lines indicate adaptive, while dashed lines are associated with uniform mesh refinements.

The implementation of the solver for the discrete problem (2.17) has been carried out in MATLAB in an extension to the short MATLAB programs [1]. The integrals of polynomials are exactly computed while numerical quadrature is utilized for the integration of non-polynomial functions, e.g., in the computation of the errors.

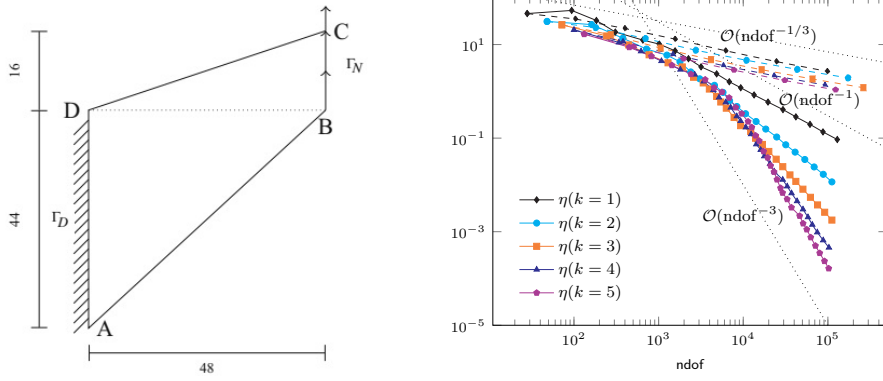


FIGURE 1. (a) Cook's membrane and (b) convergence history plot of η for $k = 1, \dots, 5$ in Subsection 5.2

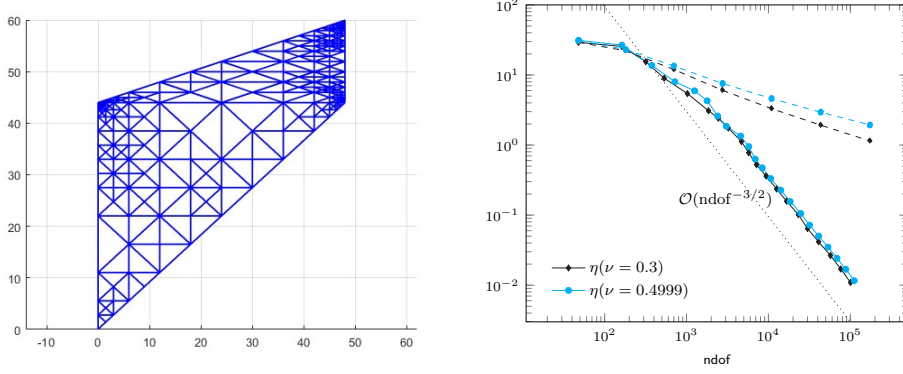


FIGURE 2. (a) Adaptive triangulation into 592 triangles generated with $k = 2$ and (b) comparison between different ν with $k = 2$ in Subsection 5.2

5.2. Cook's membrane. The tapered panel $\Omega := \text{conv}\{(0, 0), (48, 44), (48, 60), (0, 44)\}$ of Figure 1.a (courtesy from [18]) is clamped on the left-hand side $\Gamma_D := \text{conv}\{(0, 0), (0, 44)\}$, subjected to the shear load $g = (0, 1)$ in vertical direction on the right side $\{48\} \times [44, 60]$, and traction free elsewhere. The initial triangulation \mathcal{T}_0 consists of two triangles by partition of Ω along the line $[0, 48] \times \{44\}$. Figure 1.b displays the suboptimal convergence rate $1/3$ for the error estimator η with all displayed polynomial degrees $k = 1, \dots, 5$. The adaptive algorithm locally refines towards the four corners of the domain Ω in Figure 2.a for $k = 2$ and $|\mathcal{T}| = 592$ and recovers the optimal convergence rates $(k + 1)/2$ for η in Figure 1.b.

5.3. L-shaped domain. The rotated L-shaped domain $\Omega = \text{conv}\{(0, 0), (-1, -1), (0, -2), (1, -1), (2, 0), (0, 2), (-1, 1)\}$ with displayed Dirichlet and Neumann boundary parts in Figure 3.a (courtesy from [18]) allows for the exact solution u to (1.2), given in polar coordinates,

$$u_r(r, \varphi) = \frac{r^\alpha}{2\mu} (-(\alpha + 1) \cos((\alpha + 1)\varphi) + (C_2 - \alpha - 1)C_1 \cos((\alpha - 1)\varphi)),$$

$$u_\varphi(r, \varphi) = \frac{r^\alpha}{2\mu} ((\alpha + 1) \sin((\alpha + 1)\varphi) + (C_2 + \alpha - 1)C_1 \sin((\alpha - 1)\varphi))$$

with the first root $\alpha = 0.544483736782$ of $\alpha \sin(2\omega) + \sin(2\omega\alpha) = 0$ for $\omega = 3\pi/4$, $C_1 = -\cos((\alpha + 1)\omega) / \cos((\alpha - 1)\omega)$, and $C_2 = 2(\lambda + 2\mu) / (\lambda + \mu)$ [13]. The applied

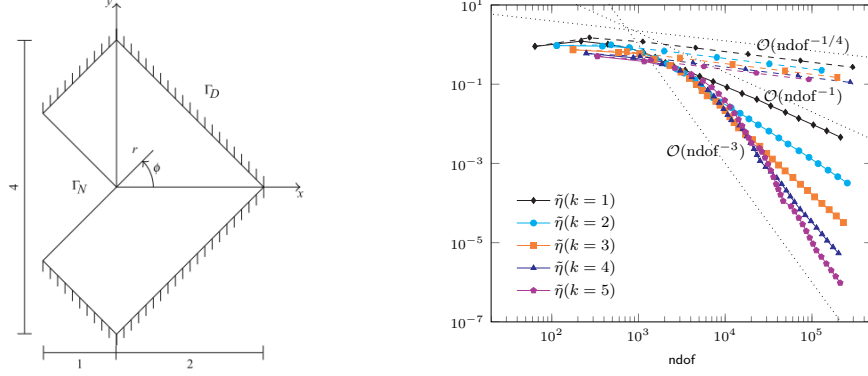


FIGURE 3. (a) Rotated L-shaped domain and (b) convergence history plot of $\tilde{\eta}$ for $k = 1, \dots, 5$ in Subsection 5.3

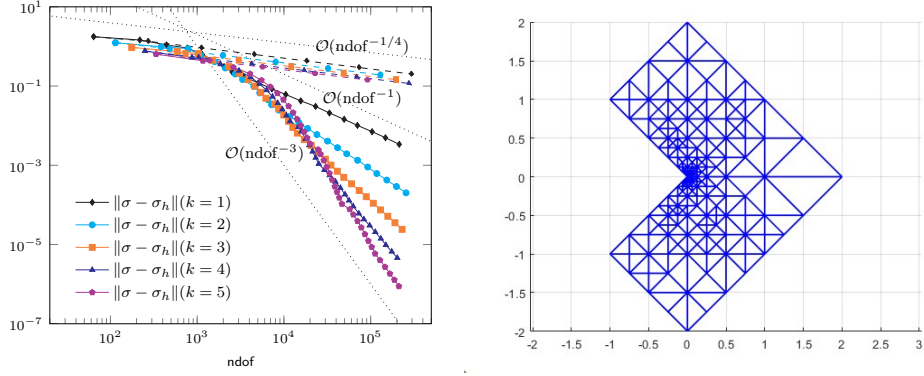


FIGURE 4. (a) Convergence history plot of $\|\sigma - \sigma_h\|$ for $k = 1, \dots, 5$ and (b) adaptive triangulation into 545 triangles generated with $k = 2$ in Subsection 5.3

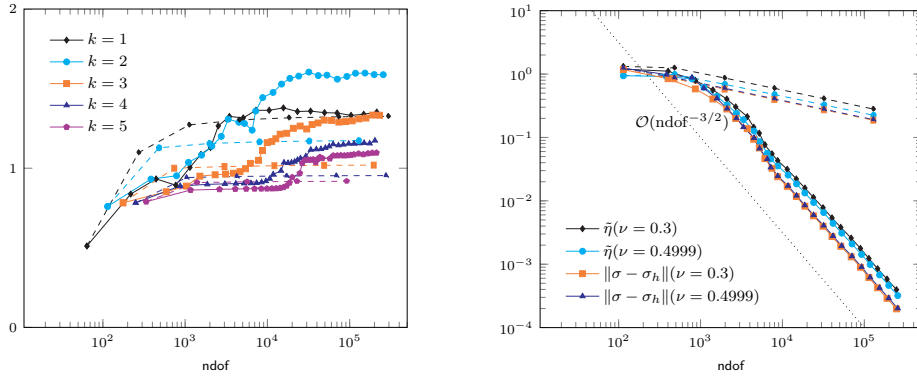


FIGURE 5. (a) Efficiency index $\tilde{\eta}/\|\sigma - \sigma_h\|$ for $k = 1, \dots, 5$ and (b) comparison between different ν with $k = 2$ in Subsection 5.3

force $f = 0$ and $g = 0$ vanish but inhomogeneous Dirichlet boundary conditions apply with $\|\sigma - \sigma_h\| \lesssim \tilde{\eta}$ from (4.17). (In particular, the local contributions of $\text{osc}(u_D, \mathcal{F}_D)^2$ are added to (5.1).)

Figure 3.b and Figure 4.a display convergence rates $1/4$ for $\tilde{\eta}$ and $\|\sigma - \sigma_h\|$ on uniform triangulations. Adaptive computations refine towards the singularity

at the origin as shown in Figure 4.b and recover the optimal convergence rates $(k + 1)/2$ for $\tilde{\eta}$ and $\|\sigma - \sigma_h\|$ with all displayed polynomial degrees k . In this example, the efficiency indices are in the range 0.5 to 2 and do not increase with larger k , cf. Figure 5.a.

5.4. Conclusions. In all three numerical examples, the a posteriori error estimator η is reliable, efficient, and λ -robust. This allows for the approximation of the Stokes equations in the incompressible limit as $\lambda \rightarrow \infty$. The adaptive algorithm driven by the local contributions of η recovers the optimal convergence rates for the approximation of singular solutions and enables higher order convergence rates in typical computational benchmarks. A comparison with the results for $\nu = 0.3$ displayed in Figure 2.b and Figure 5.b verifies empirically the λ -robustness of the method.

REFERENCES

- [1] J. Albery, C. Carstensen and S. A. Funken. Remarks around 50 lines of Matlab: short finite element implementation. *Numer. Algorithms* 20.2-3 (1999), 117–137.
- [2] D. N. Arnold and R. Winther. Mixed finite elements for elasticity. *Numer. Math.* 92.3 (2002), 401–419.
- [3] I. Babuška and M. Suri. Locking effects in the finite element approximation of elasticity problems. *Numer. Math.* 62.4 (1992), 439–463.
- [4] F. Bertrand, C. Carstensen, B. Gräßle and N. T. Tran. Stabilization-free HHO a posteriori error control. *Numer. Math.* 154.3-4 (2023), 369–408.
- [5] R. E. Bird, W. M. Coombs and S. Giani. A posteriori discontinuous Galerkin error estimator for linear elasticity. *Appl. Math. Comput.* 344/345 (2019), 78–96.
- [6] D. Boffi, F. Brezzi and M. Fortin. Mixed finite element methods and applications. Vol. 44. Springer, Heidelberg, 2013.
- [7] M. Botti, D. A. Di Pietro and A. Guglielmana. A low-order nonconforming method for linear elasticity on general meshes. *Comput. Methods Appl. Mech. Engrg.* 354 (2019), 96–118.
- [8] M. Botti, D. A. Di Pietro and P. Sochala. A hybrid high-order method for nonlinear elasticity. *SIAM J. Numer. Anal.* 55.6 (2017), 2687–2717.
- [9] D. Braess. Finite elements. Third. Theory, fast solvers, and applications in elasticity theory, Translated from the German by Larry L. Schumaker. Cambridge University Press, Cambridge, 2007, xviii+365.
- [10] S. C. Brenner. Korn’s inequalities for piecewise H^1 vector fields. *Math. Comp.* 73.247 (2004), 1067–1087.
- [11] S. C. Brenner and L. R. Scott. The mathematical theory of finite element methods. Third. Vol. 15. Springer, New York, 2008.
- [12] S. C. Brenner and L.-Y. Sung. Linear finite element methods for planar linear elasticity. *Math. Comp.* 59.200 (1992), 321–338.
- [13] C. Carstensen, M. Eigel and J. Gedicke. Computational competition of symmetric mixed FEM in linear elasticity. *Comput. Methods Appl. Mech. Engrg.* 200.41-44 (2011), 2903–2915.
- [14] C. Carstensen, D. Gallistl and M. Schedensack. L^2 best approximation of the elastic stress in the Arnold-Winther FEM. *IMA J. Numer. Anal.* 36.3 (2016), 1096–1119.
- [15] C. Carstensen and N. Nataraj. A priori and a posteriori error analysis of the Crouzeix–Raviart and Morley FEM with original and modified right-hand sides. *Comput. Methods Appl. Math.* 21.2 (2021), 289–315.
- [16] C. Carstensen and M. Schedensack. Medius analysis and comparison results for first-order finite element methods in linear elasticity. *IMA J. Numer. Anal.* 35.4 (2015), 1591–1621.
- [17] C. Carstensen and G. Dolzmann. A posteriori error estimates for mixed FEM in elasticity. *Numer. Math.* 81.2 (1998), 187–209.
- [18] C. Carstensen, D. Gallistl and J. Gedicke. Residual-based a posteriori error analysis for symmetric mixed Arnold-Winther FEM. *Numer. Math.* 142.2 (2019), 205–234.
- [19] C. Carstensen, B. Gräßle and N. Nataraj. Unifying a posteriori error analysis of five piecewise quadratic discretisations for the biharmonic equation. *J. Numer. Math.* 32.1 (2024), 77–109.
- [20] C. Carstensen and N. Heuer. A fractional-order trace-dev-div inequality. *arXiv:2403.01291* (2024).

- [21] C. Carstensen, Q. Zhai and R. Zhang. A skeletal finite element method can compute lower eigenvalue bounds. *SIAM J. Numer. Anal.* 58.1 (2020), 109–124.
- [22] M. Cicuttin, A. Ern and N. Pignet. Hybrid high-order methods—a primer with applications to solid mechanics. Springer Briefs in Mathematics. Springer, Cham, 2021, viii+136.
- [23] D. A. Di Pietro and A. Ern. A hybrid high-order locking-free method for linear elasticity on general meshes. *Comput. Methods Appl. Mech. Engrg.* 283 (2015), 1–21.
- [24] D. A. Di Pietro, A. Ern and S. Lemaire. An arbitrary-order and compact-stencil discretization of diffusion on general meshes based on local reconstruction operators. *Comput. Methods Appl. Math.* 14.4 (2014), 461–472.
- [25] D. A. Di Pietro, A. Ern, A. Linke and F. Schieweck. A discontinuous skeletal method for the viscosity-dependent Stokes problem. *Comput. Methods Appl. Mech. Engrg.* 306 (2016), 175–195.
- [26] D. A. Di Pietro and J. Droniou. The hybrid high-order method for polytopal meshes. Vol. 19. MS&A. Modeling, Simulation and Applications. Design, analysis, and applications. Springer, 2020, xxxi+525.
- [27] W. Dörfler. A convergent adaptive algorithm for Poisson’s equation. *SIAM J. Numer. Anal.* 33.3 (1996), 1106–1124.
- [28] A. Ern and J.-L. Guermond. Finite elements I—Approximation and interpolation. Vol. 72. Springer, 2021.
- [29] A. Ern and P. Zanotti. A quasi-optimal variant of the hybrid high-order method for elliptic partial differential equations with H^{-1} loads. *IMA J. Numer. Anal.* 40.4 (2020), 2163–2188.
- [30] V. Girault and P.-A. Raviart. Finite element methods for Navier-Stokes equations. Vol. 5. Theory and algorithms. Springer-Verlag, Berlin, 1986.
- [31] R. Kouhia and R. Stenberg. A linear nonconforming finite element method for nearly incompressible elasticity and Stokes flow. *Comput. Methods Appl. Mech. Engrg.* 124.3 (1995), 195–212.
- [32] C. Kreuzer and A. Veiser. Oscillation in a posteriori error estimation. *Numer. Math.* 148.1 (2021), 43–78.
- [33] P. L. Lederer and R. Stenberg. Analysis of weakly symmetric mixed finite elements for elasticity. *Math. Comp.* 93.346 (2024), 523–550.
- [34] C. Lehrenfeld. “Hybrid Discontinuous Galerkin methods for solving incompressible flow problems”. PhD thesis. Rheinisch-Westfälischen Technischen Hochschule Aachen, 2010.
- [35] J. M. Maubach. Local bisection refinement for n -simplicial grids generated by reflection. *SIAM J. Sci. Comput.* 16.1 (1995), 210–227.
- [36] D. Mora and G. Rivera. *A priori* and *a posteriori* error estimates for a virtual element spectral analysis for the elasticity equations. *IMA J. Numer. Anal.* 40.1 (2020), 322–357.
- [37] A. Rössle. Corner singularities and regularity of weak solutions for the two-dimensional Lamé equations on domains with angular corners. *J. Elasticity* 60 (2000), 57–75.
- [38] L. R. Scott and S. Zhang. Finite element interpolation of nonsmooth functions satisfying boundary conditions. *Math. Comp.* 54.190 (1990), 483–493.
- [39] R. Stevenson. The completion of locally refined simplicial partitions created by bisection. *Math. Comput.* 77.261 (2008), 227–241.
- [40] A. Veiser and P. Zanotti. Quasi-optimal nonconforming methods for symmetric elliptic problems. II—Overconsistency and classical nonconforming elements. *SIAM J. Numer. Anal.* 57.1 (2019), 266–292.
- [41] A. Veiser and P. Zanotti. Quasi-optimal nonconforming methods for symmetric elliptic problems. III—Discontinuous Galerkin and other interior penalty methods. *SIAM J. Numer. Anal.* 56.5 (2018), 2871–2894.
- [42] L. Beirão da Veiga, F. Brezzi, L. D. Marini and A. Russo. The virtual element method. *Acta Numer.* 32 (2023), 123–202.
- [43] L. Beirão da Veiga, C. Canuto, R. H. Nochetto, G. Vacca and M. Verani. Adaptive VEM: stabilization-free a posteriori error analysis and contraction property. *SIAM J. Numer. Anal.* 61.2 (2023), 457–494.
- [44] R. Verfürth. A posteriori error estimation techniques for finite element methods. Oxford University Press, Oxford, 2013.

(C. Carstensen) HUMBOLDT-UNIVERSITÄT ZU BERLIN, 10117 BERLIN, GERMANY
Email address: cc@math.hu-berlin.de

(N. T. Tran) UNIVERSITÄT AUGSBURG, 86159 AUGSBURG, GERMANY
Email address: ngoc1.tran@uni-a.de